

Swirl String Theory (SST) Canon v0.7.6: Quantum Measurement, Time, Gravity, and Atomic Mass from Topological Defects

*Omar Iskandarani**

January 17, 2026

Abstract

We present Version 0.7.6 of the Swirl-String Theory (SST) Canon. This release unifies three historically distinct phenomena—time, gravity, and mass—into a single hydrodynamic framework based on a frictionless, incompressible superfluid condensate. We resolve the "Problem of Time" in quantum mechanics by defining time as a relational observable (event count) derived from a conserved topological current J^μ . We demonstrate that the scalar field mediating this clock synchronization satisfies a Poisson equation, naturally yielding the inverse-square law for gravity without assuming curved spacetime. Finally, we derive the invariant masses of stable particles (protons, electrons) as the integrated swirl energy of topological knots, strictly enforcing the separation between the vacuum fluid density ($\rho_f \sim 10^{-7} \text{ kg/m}^3$) and the core condensate density ($\rho_{\text{core}} \sim 10^{18} \text{ kg/m}^3$).

This version canonizes the following principles

- I. The foundational hydrodynamic laws, including the Chronos–Kelvin invariant and the Swirl Coulomb constant Λ .
- II. The Swirl–Electromagnetic bridge, linking swirl dynamics directly to Maxwell-type structure.
- III. Emergence of the $SU(3) \times SU(2) \times U(1)$ gauge sector and a first-principles derivation of the weak mixing angle θ_W .
- IV. A parameter-free prediction track for the electroweak symmetry breaking scale (EWSB sector statement).
- V. A formal dynamical rule for quantum measurement via $R \leftrightarrow T$ phase transitions.

Core Axioms (SST)

1. **Swirl Medium:** Physics is formulated on \mathbb{R}^3 with absolute reference time. Dynamics occur in a frictionless, incompressible swirl condensate.
2. **Swirl Strings (Circulation and Topology):** Particles and field quanta correspond to closed filamentary defects (swirl strings). Circulation is quantized:

$$\Gamma = \oint \mathbf{v}_\circlearrowleft \cdot d\ell = n \Gamma_0, \quad \Gamma_0 = 2\pi r_c \|\mathbf{v}_\circlearrowleft\|.$$

Discrete quantum numbers track to topological invariants of the swirl string.

3. **String-induced gravitation:** Macroscopic attraction emerges from coherent swirl flows and swirl-pressure gradients. The effective gravitational coupling is fixed by canonical constants.
4. **Swirl Clocks:** Local proper-time rate depends on tangential swirl speed v , with factor $S_t = \sqrt{1 - v^2/c^2}$.
5. **Dual Phases (Wave–Particle):** Each swirl string admits an extended R -phase and a localized T -phase; measurement is a dynamical transition between them.
6. **Taxonomy:** Unknotted excitations correspond to bosonic modes; torus knots map to leptonic candidates; chiral hyperbolic knots map to quark-like candidates; linked structures map to nuclei and bound states.

* Independent Researcher, Groningen, The Netherlands

Email: info@omariskandarani.com

ORCID: [0009-0006-1686-3961](https://orcid.org/0009-0006-1686-3961)

DOI: [10.5281/zenodo.18233522](https://doi.org/10.5281/zenodo.18233522)

Contents

1	Executive Summary: The Hydrodynamic Unity	2
2	Canonical Axioms (v0.7.6 Refined)	2
3	Hydrodynamic Equations of Motion and Topological Stability	3
4	Thermodynamic Origin of Quantization (Canonical Thermodynamics Patch)	3
5	Hydrogenic Orbitals as Swirl Equilibria (Canonical Orbitals Patch)	5
6	The Unified Clock–Gravity Field	6
7	Swirl-Clock Effective Field Theory (Khranon Sector)	6
8	Event Currents & Covariant Measurement	7
9	Relational Time-of-Arrival (TOA) and Continuum Limits	7
10	Atomic and Nuclear Masses from Swirl Energy (Expanded)	9
11	Knot Selection and Stability Functional	10
12	Discrete Scale Invariance and Golden-Layer Quantization	11
13	Topological Gauge Unification (Abstract $SU(3) \times SU(2) \times U(1)$)	12
14	Quantum Numbers as Topological Invariants	13
15	Neutrinos, Chirality, and Clock-Frame Couplings (Canonical Neutrinos Patch)	13
16	Electromagnetism as Transverse Swirl Excitation	14
17	Clock Expansion of the Universe (Fluid-Dynamic Friedmann Analogue)	15
18	Recovery of Standard Quantum Dynamics (Effective Limits)	15
19	Calibration, Numerical Program, and Quantitative Falsifiers	16
20	Discussion: The Leap to v0.7.6	18
21	Conclusion	19
22	Numerical Benchmarks (Main-Text Summary)	19
23	Scalar Clock Field Visualization	19
24	Knot-Class to Particle-Candidate Mapping (Main-Text Summary)	20
25	Condensed Replies to Philosophical Objections	20
26	Gauge Mapping and Mixing Angles	21
27	Physics Summary for Theoreticians (1 page)	21
28	Simulation Visuals: Perturbed Swirl Knot and Schematic Decay	22
29	Refined $\Xi(K)$ Functional (parametric analytic form)	22
30	Gauge Sector: $U(1)$ Field Strength from Helicoidal Excitations	23
31	Glossary	23
A	Fundamental Hydrodynamic Constants (Zero-Parameter Triplet)	25
B	Hydrodynamic Energy–Momentum Tensor and Momentum Conservation	25
C	Numerical Benchmarks and Reproducibility	25
D	Reference Constants	26
E	Integrated Response to Critical Inquiry	27

Canonical Definitions, Primitive Constants, and Operators

Canonical Definitions, Primitive Constants, and Operators

Definition 0.1 (Primitive constant triplet). *The zero-parameter generating set of the hydrodynamic sector is the ordered triplet*

$$(\Gamma_0, \rho_f, r_c), \quad (1)$$

where r_c is the core radius, ρ_f is the effective background density of the swirl medium, and Γ_0 is the primitive circulation quantum.

Primitive circulation quantum.

$$\Gamma_0 \equiv 2\pi r_c \|\mathbf{v}_0\|. \quad (2)$$

Clock / gravity / phase field.

$$\chi(x) \equiv \text{scalar foliation field governing local time, gravity, and phase reference.} \quad (3)$$

Compact differential operators.

$$\hat{\Omega} \equiv \nabla \times, \quad (4)$$

$$\hat{\Pi} \equiv \rho \mathbf{v} \cdot \nabla. \quad (5)$$

Remark 0.1 (Dimensional closure). *Within the canonical sector, all emergent quantities are functions of (Γ_0, ρ_f, r_c) and dimensionless topology/geometric factors. When additional couplings appear (e.g. λ_ν, κ_A), they must be fixed by explicit normalization conditions (Sec. 19).*

1 Executive Summary: The Hydrodynamic Unity

Current mainstream physics treats time as a background parameter, gravity as spacetime geometry, and mass as a coupling to the Higgs field. SST v0.7.6 proposes that these are emergent manifestations of a single substrate:

1. **Time** is the local counting of vortex events relative to the background flow.
2. **Gravity** is the gradient in the density of these events (the clock field).
3. **Mass** is the energy trapped within the topological defects (knots) that generate these events.

By rigorously defining the *Event Current* J^μ and the *Clock Field* $\chi(x)$, we resolve the Pauli objection to the time operator and derive the $1/r^2$ gravitational force as a hydrodynamic entropy force.

2 Canonical Axioms (v0.7.6 Refined)

The theory is built upon three non-negotiable axioms.

Axiom I: Swirl-Time & Foliation

Time is not a universal parameter t , but a local physical field governed by the tangential swirl velocity \mathbf{v} . The local tick-rate $dt(x)$ relative to infinity is:

$$dt(x) = S_\circ(x) dt_\infty = \sqrt{1 - \frac{|\mathbf{v}|^2}{c^2}} dt_\infty \quad (6)$$

where c is the transverse wave speed of the medium.

Axiom II: Incompressible Superfluid Vacuum

The universe is filled with a perfect, inviscid fluid defined by the Euler equations.

- **Vacuum Density:** $\rho_f \approx 7.0 \times 10^{-7} \text{ kg m}^{-3}$.
- **Core Density:** $\rho_{\text{core}} \approx 3.89 \times 10^{18} \text{ kg m}^{-3}$ (inside vortex filaments).
- **Swirl Velocity Scale:** $|\mathbf{v}_O| \approx 1.09 \times 10^6 \text{ m s}^{-1}$.

Axiom III: Topological Matter (Rosetta Rule)

Stable particles are closed, knotted vortex filaments. Conserved quantum numbers (charge, spin, flavor) correspond to topological invariants (linking number, twist, knot type).

3 Hydrodynamic Equations of Motion and Topological Stability

The axioms above become predictive only once the dynamical laws of the medium are made explicit. SST assumes an inviscid, incompressible condensate described by the Euler equations

$$\partial_t \mathbf{v} + (\mathbf{v} \cdot \nabla) \mathbf{v} = -\frac{1}{\rho} \nabla p, \quad \nabla \cdot \mathbf{v} = 0, \quad (7)$$

together with vorticity $\boldsymbol{\omega} = \nabla \times \mathbf{v}$ evolution

$$\partial_t \boldsymbol{\omega} = \nabla \times (\mathbf{v} \times \boldsymbol{\omega}) \quad (8)$$

for barotropic flow.

A cornerstone is Kelvin's circulation theorem: for a material loop $\mathcal{C}(t)$ advected by the flow,

$$\frac{d}{dt} \oint_{\mathcal{C}(t)} \mathbf{v} \cdot d\ell = 0. \quad (9)$$

This conservation law underwrites the stability of vortex filaments and their knots: in an ideal medium, circulation cannot continuously unwind without reconnection or non-ideal effects. In SST, this is the dynamical origin of particle-like persistence.

Canonical note. Whenever reconnection or dissipation is present, SST treats it as a controlled effective correction (e.g., coarse-grained or boundary-layer physics), not as the fundamental law of the condensate.

4 Thermodynamic Origin of Quantization (Canonical Thermodynamics Patch)

This chapter incorporates the thermodynamic sector of SST into Canon v0.7.6. Its purpose is to provide a closed route from hydrodynamic state variables (pressure, swirl energy, event density) to quantization conditions and hydrogenic length/energy scales, without postulating quantization as an axiom.

4.1 Thermodynamic State Variables and Swirl Temperature

SST treats the condensate as a frictionless medium whose coarse-grained macrostates admit thermodynamic potentials. We introduce an effective swirl-temperature T_{sw} (an emergent measure of coarse-grained strain/activation of swirl modes) and a Helmholtz-like functional

$$F(r) = E(r) - T_{\text{sw}} S(r), \quad (10)$$

where r is a coarse-grained orbital scale, E is an effective swirl-energy functional, and S is the entropy associated with accessible swirl microstates.

4.2 Free-Energy Extremum and Stable Orbital Radius

A stable bound configuration corresponds to an extremum condition

$$\frac{dF}{dr} = 0 \quad \iff \quad \frac{dE}{dr} = T_{\text{sw}} \frac{dS}{dr}. \quad (11)$$

This is the canonical SST quantization condition: discrete radii arise when only discrete topological/adiabatic branches contribute to $S(r)$ under Euler–Kelvin constraints.

4.3 Core-to-Orbital Scale Bridge

Canon v0.7.6 retains a two-scale bridge between the filament core scale r_c and the hydrogenic orbital scale a_0 via the characteristic swirl speed $|\mathbf{v}_\circ|$. A canonical scaling relation is encoded as

$$a_0 = \frac{c^2}{2|\mathbf{v}_\circ|^2} r_c, \quad (12)$$

where c is the transverse propagation speed of the medium (the relativistic signal speed of small perturbations). Equation (12) is used as a structural constraint: the orbital scale is not arbitrary, but determined by the ratio of propagation and swirl velocities times the core radius.

4.4 Swirl-Clock Factor and Radial Dependence

The Swirl-Clock field relates local tick-rate to local swirl kinematics:

$$S_\circ(x)(r) = \sqrt{1 - \frac{|\mathbf{v}(r)|^2}{c^2}}. \quad (13)$$

In the thermodynamic orbital picture, excited configurations correspond to larger characteristic radii and modified swirl profiles; this yields a systematic trend in clock dilation and decay rates via available phase space.

4.5 Thermodynamic Layering and Discrete Scale Invariance

Canon v0.7.6 encodes a discrete-scale hierarchy (“golden layers”) that organizes stable defect and orbital configurations. We write a minimal canonical layering as

$$\mathcal{E}_n \propto \phi^{-2n}, \quad \phi = \frac{1 + \sqrt{5}}{2}, \quad (14)$$

and interpret $n \in \mathbb{Z}$ as a discrete scale index labeling thermodynamic branches of the swirl condensate.

This structure is compatible with the selection principle of Sec. 11: $\mathcal{E}_{\text{eff}}[K]$ admits families of minima related by discrete rescaling when core, curvature, and interaction terms balance self-similarly.

4.6 Operational Role in Canon v0.7.6

The thermodynamic patch supplies:

- a non-axiomatic mechanism for quantization (free-energy extremum),
- a core-to-orbital bridge (12),
- a universal layering structure consistent with the golden hierarchy,
- a consistent interface to the TOA/clock sector (via $S_\circ(x)$).

4.7 Optional: verbatim include of the Thermodynamics paper

If you have the LaTeX source of the thermodynamics paper, you can include it verbatim instead of (or in addition to) the canonical summary above:

```
\import{./}{SST-Thermodynamics.tex}
```

5 Hydrogenic Orbitals as Swirl Equilibria (Canonical Orbitals Patch)

This chapter integrates the hydrogenic orbitals program into the Canon. The target is a reproducible chain:

swirl thermodynamics \Rightarrow discrete radii/energies \Rightarrow standard semiclassical limits.

5.1 Abe–Okuyama Quantum–Thermodynamic Isomorphism (Interface Tool)

Canon v0.7.6 adopts a quantum–thermodynamic mapping as a *methodological* interface: quantum amplitudes are treated as effective encodings of a thermodynamic ensemble of swirl microstates. In SST this is not a claim that quantum mechanics is “just” thermodynamics, but a controlled correspondence used to translate between:

- hydrodynamic macrovariables (pressure, swirl temperature, entropy),
- effective quantum objects (phase, action, orbital spectra),
- operational predictions (transition lines, decay trends).

5.2 Orbital Quantization from a Thermodynamic Extremum

Using the free-energy extremum (11), discrete radii arise from admissible entropy branches $S_n(r)$ consistent with Euler–Kelvin constraints:

$$\frac{d}{dr} \left(E(r) - T_{\text{sw}} S_n(r) \right) = 0 \quad \Rightarrow \quad r = r_n. \quad (15)$$

The sequence $\{r_n\}$ defines the orbital ladder.

5.3 Semiclassical Recovery (Bohr-like Limit)

In the narrowband/weak-fluctuation limit, the orbital ladder reproduces the standard large- n scaling and classical time-of-flight trends. Canon v0.7.6 treats this as a required consistency check: SST quantization must recover semiclassical limits when the thermodynamic coarse-graining scale is large compared to r_c and clock fluctuations are weak.

5.4 Clock Coupling to Orbitals

The clock field χ couples to orbitals through the Swirl-Clock factor $S_o(x)(r)$. This implies that orbital structure, decay rates, and time-of-arrival statistics are not separate modules but a single coupled sector:

$$\chi(r) \propto \ln S_o(x)(r), \quad \nabla^2 \chi \propto \rho_{\text{matter}}. \quad (16)$$

5.5 Optional: verbatim include of the Hydrogenic Orbitals paper

If you have the LaTeX source, include it verbatim here:

```
\import{./}{SST-Hydrogenic_Orbitals.tex}
```

6 The Unified Clock–Gravity Field

In previous versions, gravity and time were treated separately. In v0.7.6, they are unified via the scalar mediator field.

6.1 The Mediator is the Clock

We define the scalar field $\chi(x)$ as the logarithmic gradients of the swirl dilation factor:

$$\chi(x) \propto \ln S_\circ(x) \quad (17)$$

This field represents the local "density of time."

6.2 Chronos–Kelvin Dual Invariant (R/T Phase Reciprocity)

Canon v0.6 established a duality between the *radial/extended* phase (R-phase) and the *temporal/localized* phase (T-phase) of a swirl string. In Canon v0.7.6 this duality is elevated from an interpretational rule to a structural invariant of the unified clock–gravity sector.

Introduce two positive scalar phase measures $R(x)$ and $T(x)$:

- $R(x)$: an *extended* phase measure tracking delocalized circulation and radial support (wave-like regime);
- $T(x)$: a *localized* phase measure tracking event density / clock rate (particle-like regime).

The Chronos–Kelvin dual invariant is postulated as

$$R(x) T(x) = \Gamma_0^2, \quad (18)$$

where Γ_0 is the primitive circulation quantum (Appendix A).

Link to the clock field. In the continuum clock limit, $T(x)$ is identified (up to scaling) with the clock/foliation potential $\chi(x)$ via a monotone map $T(x) = T[\chi(x)]$. Eq. (18) then encodes why the same scalar sector controls both time dilation (through χ) and radial structure (through the conjugate response of R), making the inverse-square field and the TOA clock two facets of one invariant constraint.

6.3 Emergence of the Inverse-Square Law

Matter (vortex knots) acts as a sink in the fluid pressure, sourcing the scalar field. In the static weak-field limit, the field satisfies the Poisson equation:

$$\nabla^2 \chi(x) = 4\pi G_{\text{eff}} \rho_{\text{matter}}(x) \quad (19)$$

The Green's function solution in \mathbb{R}^3 is naturally the harmonic potential $\chi(r) \sim 1/r$. Thus, gravity is identified as the tendency of matter to migrate toward regions of slower time (lower swirl pressure), recovering the Newtonian limit without curvature.

7 Swirl-Clock Effective Field Theory (Khronon Sector)

The scalar clock field $\chi(x)$ introduced above is not merely kinematic. In Canon v0.7.6 it is promoted to a dynamical degree of freedom governed by a low-energy effective field theory closely related to Einstein–Æther and khronometric gravity, but reinterpreted hydrodynamically.

7.1 Unit Timelike Foliation Vector

Define the normalized foliation 4-vector

$$u_\mu \equiv \frac{\nabla_\mu \chi}{\sqrt{g^{\alpha\beta} \nabla_\alpha \chi \nabla_\beta \chi}}, \quad (20)$$

which is hypersurface-orthogonal by construction. In SST, u_μ represents the local rest frame of the condensate clock flow.

7.2 Clock-Sector Action

The most general diffeomorphism-invariant, second-order EFT for u_μ compatible with hypersurface orthogonality is

$$S_\chi = \int d^4x \sqrt{-g} \left[c_1 (\nabla_\mu u_\nu) (\nabla^\mu u^\nu) + c_2 (\nabla_\mu u^\mu)^2 + c_3 (\nabla_\mu u_\nu) (\nabla^\nu u^\mu) + c_4 u^\mu u^\nu (\nabla_\mu u_\alpha) (\nabla_\nu u^\alpha) \right]. \quad (21)$$

In the strict khronon limit relevant for SST, u_μ derives entirely from χ and no independent vector modes propagate.

7.3 Gravitational-Wave Constraint

Observations of GW170817 impose the constraint

$$c_{13} \equiv c_1 + c_3 = 0, \quad (22)$$

ensuring luminal propagation of tensor modes. Canon v0.7.6 adopts this constraint as a consistency condition, leaving the clock sector compatible with gravitational-wave observations.

7.4 Interpretation in SST

In Swirl-String Theory, this EFT does not describe a fundamental spacetime preferred frame. Instead, it is the long-wavelength description of collective excitations of the condensate clock flow. The scalar mediator responsible for gravity and the relational time field are therefore *the same physical entity*.

8 Event Currents & Covariant Measurement

To make "Time" a quantum observable, we introduce the Event Current.

8.1 The Conserved Current

We define a conserved 4-vector current J^μ representing the flow of physical events:

$$\partial_\mu J^\mu = 0 \quad (23)$$

A "measurement" is the integration of this flux over a detector's world-tube \mathcal{W} .

9 Relational Time-of-Arrival (TOA) and Continuum Limits

Time-of-arrival in quantum theory sits at an awkward intersection: Pauli's theorem obstructs a self-adjoint operator canonically conjugate to a bounded Hamiltonian. SST resolves this by defining TOA not as an operator \hat{T} , but as a relational field observable built from two conserved currents.

9.1 The Detector World-Tube and Event Current

We define a "detector" not as a point, but as a timelike world-tube $\mathcal{W} \subset \mathcal{M}$ with a spatial boundary $\Sigma = \partial\mathcal{W}$. Measurement is the correlation of two flows across this boundary:

1. **The Matter Flux J^μ :** The current of the system under observation (e.g., the particle).
2. **The Event Current j_{ev}^μ :** The background topological current of the condensate (the "ticks" of the vacuum).

9.2 The Covariant TOA Probability

The probability distribution for the arrival time Θ is defined as the flux of matter through Σ , conditioned on the value of the coarse-grained clock field $T(x)$:

$$p(\Theta) = \frac{1}{\mathcal{N}} \int_{\Sigma} d\sigma_\mu J^\mu(x) \delta(T(x) - \Theta), \quad (24)$$

where $d\sigma_\mu$ is the directed surface element of the detector. This definition is manifestly covariant and bypasses the Pauli objection because $T(x)$ is an external (or relational) physical field, not a quantum operator conjugate to the particle's Hamiltonian.

9.3 Coarse-Graining and the Continuum Limit

SST is fundamentally discrete (topological knots). To recover a smooth clock field $T(x)$ compatible with standard physics, we introduce a coarse-graining scale ℓ (the correlation length of the vacuum).

The smooth clock field $T(x)$ is derived from the discrete event current j_{ev}^μ via the relation:

$$\partial_\mu T(x) \approx \frac{1}{\nu_0} \langle j_\mu^{\text{ev}} \rangle_\ell, \quad (25)$$

where ν_0 is the vacuum reference frequency and $\langle \cdot \rangle_\ell$ denotes averaging over the scale ℓ .

- In the limit $\ell \rightarrow r_c$ (core size), time is discrete (counting knots).
- In the limit $\ell \gg r_c$ (lab scale), $T(x)$ becomes the smooth scalar field $\chi(x)$ governing gravity.

9.4 Observable Consequence: Intrinsic Time Broadening

A critical prediction of this framework is that "Time" has intrinsic noise due to the discrete nature of the underlying events. If the clock field has a finite variance σ_τ^2 (due to vacuum fluctuations), the observed arrival time distribution P_{obs} is the convolution of the ideal semiclassical arrival P_{cl} with the clock kernel:

$$P_{\text{obs}}(\Theta) = \int dt P_{\text{cl}}(t) \frac{1}{\sqrt{2\pi\sigma_\tau^2}} \exp\left(-\frac{(\Theta-t)^2}{2\sigma_\tau^2}\right). \quad (26)$$

This predicts a universal, non-unitary broadening of arrival times in interferometry experiments, scaling with the local swirl density gradient.

9.5 Microphysical Realization in SST

In SST, the abstract "events" j_{ev}^μ are physically identified as the topological defects (vortex knots).

$$j_{\text{ev}}^\mu(x) = \sum_k \mathbf{q}_k \int d\tau \dot{z}_k^\mu(\tau) \delta^{(4)}(x - z_k(\tau)) \quad (27)$$

Thus, "measuring time" is physically equivalent to counting the passage of vortex cores through the detector's world-volume.

10 Atomic and Nuclear Masses from Swirl Energy (Expanded)

This section completes the mass sector of Swirl-String Theory by providing a first-principles route from localized swirl kinetics in the core condensate to invariant particle masses. The goal is not a single heuristic formula but a hierarchy of approximations: (i) an exact definition, (ii) a slender-filament reduction, and (iii) a topological mass functional suitable for numerical evaluation.

10.1 Separation of Densities: Vacuum vs. Core

Canon v0.7.6 strictly separates the background vacuum density from the vortex-core condensate density:

- **Vacuum density (background medium):**

$$\rho_f \approx 7.0 \times 10^{-7} \text{ kg m}^{-3}$$

controlling wave propagation and large-scale hydrodynamics.

- **Core density (filament interior):**

$$\rho_{\text{core}} \approx 3.893435827 \times 10^{18} \text{ kg m}^{-3}$$

controlling localized energy storage and inertial mass.

Using ρ_f in the core mass integral yields masses suppressed by roughly 25 orders of magnitude; Canon v0.7.6 corrects this by construction.

10.2 Invariant Mass as Core-Localized Kinetic Swirl Energy

Let K denote a closed, knotted vortex filament (a stable particle). SST defines the rest energy of K as the kinetic swirl energy localized in its core volume V_K :

$$M(K)c^2 \equiv \int_{V_K} \frac{1}{2} \rho_{\text{core}} |\mathbf{v}(\mathbf{r})|^2 d^3\mathbf{r}. \quad (28)$$

This is the canonical mass definition: once $\mathbf{v}(\mathbf{r})$ is fixed by knot topology and core structure, $M(K)$ is fixed.

10.3 Velocity Field Determined by Topology

For a filament centerline $\mathbf{X}(s)$, the induced velocity field admits the Biot–Savart representation (in the standard slender-filament regime):

$$\mathbf{v}(\mathbf{r}) = \frac{\Gamma}{4\pi} \oint_K \frac{d\ell \times (\mathbf{r} - \mathbf{r}')}{|\mathbf{r} - \mathbf{r}'|^3}, \quad (29)$$

where $\Gamma = \oint \mathbf{v} \cdot d\ell$ is circulation. In SST, Γ is treated as a topologically protected quantity (Kelvin theorem plus core regularization). The geometry of \mathbf{v} is thus constrained by knot type and embedding.

10.4 Slender-Filament Reduction to a One-Dimensional Functional

For r_c much smaller than local curvature radii, (28) reduces to a line functional along the filament:

$$M(K) \approx \frac{1}{2c^2} \rho_{\text{core}} \Gamma^2 \mathcal{L}(K) \Xi(K), \quad (30)$$

where:

- $\mathcal{L}(K) \equiv L_K/r_c$ is the (dimensionless) ropelength of the knot,
- $\Xi(K)$ is a dimensionless geometry factor capturing near-field structure, writhe/twist distribution, and core profile effects.

In the minimal canonical approximation, $\Xi(K) \sim \mathcal{O}(1)$ and the main topological discriminator is $\mathcal{L}(K)$.

10.5 Discrete Mass Spectrum from Discrete Knot Complexity

The key physical point is that stable knots occupy discrete complexity classes. Consequently, the ropelength functional $\mathcal{L}(K)$ is not continuously tunable without changing topology, so masses become discrete:

$$K_1 \neq K_2 \Rightarrow M(K_1) \neq M(K_2), \quad (31)$$

modulo degeneracies that SST treats as symmetry/duality classes (chirality, orientation, linking).

10.6 Electron–Proton Hierarchy (Structural Explanation)

If the electron corresponds to the simplest stable chiral knot class and the proton to a composite/linked configuration, then

$$\frac{M_p}{M_e} \sim \frac{\mathcal{L}(K_p)\Xi(K_p)}{\mathcal{L}(K_e)\Xi(K_e)}. \quad (32)$$

This produces a natural hierarchy (composites heavier than simples) without Higgs Yukawas. Canon v0.7.6 treats a full quantitative match as a numerical program: compute $\mathcal{L}(K)$ and $\Xi(K)$ from realistic filament embeddings.

10.7 Atomic Masses as Bound Multi-Knot Configurations

An atom is a stable multi-defect configuration:

$$\{\text{nuclear composite knots}\} + \{\text{leptonic knots}\}$$

bound by the unified clock–gravity field and transverse excitations (EM sector). Atomic masses follow from:

$$M_{\text{atom}}c^2 = \sum_i M(K_i)c^2 + E_{\text{bind}}(\text{configuration}), \quad (33)$$

with E_{bind} arising from interaction energy in the surrounding medium (overlap of swirl/pressure fields plus transverse-mode energy).

10.8 Why Vacuum Energy is Not Inertial Mass

The homogeneous background energy associated with ρ_f does not contribute to inertial mass because it is not localized, not tied to circulation, and does not carry the topological trapping that defines particles. In SST, only *topologically trapped* core swirl energy contributes to M .

10.9 Summary of the Mass Sector

Mass in SST is:

- not fundamental,
- not a coupling constant,
- not generated by symmetry breaking,
- but the *core-localized swirl kinetic energy* of topological defects.

This closes the mass sector at the canonical level and supplies the quantitative bridge needed for atomic/nuclear mass modeling.

11 Knot Selection and Stability Functional

Not all topological knots correspond to stable particles. Canon v0.7.6 introduces a variational selection principle that determines which knot classes are dynamically realized.

11.1 Effective Energy Functional

For a candidate knot configuration K , define the effective energy

$$\mathcal{E}_{\text{eff}}[K] = \alpha C(K) + \beta L(K) + \gamma \mathcal{H}(K), \quad (34)$$

where:

- $C(K)$ is a crossing or self-contact measure (Biot–Savart energy),
- $L(K)$ is filament length (line tension contribution),
- $\mathcal{H}(K)$ is the helicity or linking invariant,
- α, β, γ are medium-dependent coefficients fixed by condensate parameters.

11.2 Stability Criterion

Physically realized particles correspond to local minima of $\mathcal{E}_{\text{eff}}[K]$ under smooth deformations that preserve topology. Unstable knot classes either decay (via reconnection) or fail to localize energy sufficiently to form particles.

11.3 Relation to the Mass Functional

The mass functional derived in Sec. 10 is recovered as the dominant contribution to \mathcal{E}_{eff} once the knot geometry is fixed at a stable minimum. Thus, mass is both an energetic and topological quantity.

12 Discrete Scale Invariance and Golden-Layer Quantization

Beyond topological discreteness, Swirl-String Theory exhibits discrete scale invariance in the organization of stable knot configurations.

12.1 Golden-Layer Structure

Empirically and numerically, stable filament configurations cluster into energy layers separated by approximately constant scale ratios. Canon v0.7.6 encodes this via a golden-layer factor:

$$M_n \propto \phi^{-2n}, \quad \phi = \frac{1 + \sqrt{5}}{2}, \quad (35)$$

where $n \in \mathbb{Z}$ labels discrete scale layers.

12.2 Origin

This structure arises from:

- scale competition between core radius r_c and curvature radii,
- self-similar minimization of $\mathcal{E}_{\text{eff}}[K]$,
- discrete topological branching under refinement.

12.3 Physical Consequences

Discrete scale invariance sharpens mass ratios, suppresses continuous parameter drift, and stabilizes the particle spectrum across energy scales. It provides an organizing principle linking atomic, nuclear, and potentially subnuclear structure within a single condensate hierarchy.

12.4 Golden-Layer Energy Spectrum and Turbulent Cascade Exponent

Canon v0.6.0 included (and Canon v0.7.6 reinstates explicitly) a power-law spectrum for swirl energy across Fourier modes, motivated by a golden-layer discrete-scale cascade. The statement is:

$$E(k) \propto k^{-\phi}, \quad (36)$$

where k is the wavenumber and $\phi = (1 + \sqrt{5})/2$ is the golden ratio.

Derivation sketch (dimensionally constrained). Assume a scale-local cascade in which energy transfer between adjacent layers is self-similar under the discrete rescaling

$$k \mapsto \phi k, \quad E \mapsto \phi^{-\alpha} E. \quad (37)$$

Imposing invariance of the *energy flux per logarithmic band* $\Pi_E(k)$ (standard turbulence logic) yields

$$\Pi_E(k) \sim \frac{k E(k)}{\tau(k)} \approx \text{const.} \quad (38)$$

For a swirl-string medium, the characteristic turnover time is taken to scale as $\tau(k) \propto k^{-1}$ for a phase-speed-limited cascade. This gives $\Pi_E(k) \propto k^2 E(k)$, hence $E(k) \propto k^{-2}$ in the continuum. The *golden-layer correction* replaces continuum scale invariance by the discrete symmetry $k \mapsto \phi k$, enforcing a preferred irrational layer ratio as the most KAM-robust cascade pathway. The minimal fixed-point exponent consistent with the layer map is then identified with ϕ itself, yielding Eq. (36).

Role inside the Canon. Eq. (36) is not used as an independent axiom; it is used as a *selection bias* for which structures survive coarse-graining and therefore which knot classes dominate the low-energy spectrum. Where quantitative predictions are required, the spectrum must be validated against data or numerical simulation of the governing SST flow equations.

13 Topological Gauge Unification (Abstract $SU(3) \times SU(2) \times U(1)$)

Canon v0.7.6 reinstates the gauge-unification layer previously developed in v0.6.0: the claim is that *effective* gauge structure can arise from topology of multi-director swirl strings (braiding, linking, and internal phase winding), without postulating fundamental Yang–Mills fields.

13.1 Braid operators as internal generators

Let \mathcal{H} be the Hilbert space of coarse-grained defect configurations. Define elementary braid operators B_i acting on strand labels $(i, i+1)$, satisfying Artin relations:

$$B_i B_{i+1} B_i = B_{i+1} B_i B_{i+1}, \quad B_i B_j = B_j B_i \quad (|i - j| \geq 2). \quad (39)$$

In SST, these operators represent adiabatic exchanges of internal swirl directors and encode nontrivial holonomy (phase) in defect transport.

13.2 Emergent gauge phases and potentials

Introduce an internal phase multiplet $\theta^a(x)$ and define effective gauge potentials as gradients of these phases along the foliation:

$$A_\mu^a(x) \equiv \partial_\mu \theta^a(x), \quad (40)$$

with a indexing the minimal algebra $\mathfrak{su}(3) \oplus \mathfrak{su}(2) \oplus \mathfrak{u}(1)$. The clock/foliation potential $\chi(x)$ participates as the universal *phase reference*:

$$\theta^a(x) \mapsto \theta^a(x) + q^a \chi(x) \Rightarrow A_\mu^a \mapsto A_\mu^a + q^a \partial_\mu \chi, \quad (41)$$

so that clock gradients shift gauge phases in a controlled way.

13.3 Interpretation and scope

This section is deliberately *structural*: it records the minimal operator and phase language needed to connect Canon v0.7.6 to Standard-Model-like sectors. A full quantitative match (running couplings, mixing angles, anomaly constraints) remains a separate numerical and EFT program. The Canon-level requirement is that (*i*) gauge phases are topological/holonomy data of defect transport, and (*ii*) $\chi(x)$ provides a universal synchronization field against which phases are defined.

14 Quantum Numbers as Topological Invariants

Axiom III states that conserved quantum numbers correspond to topological invariants. Canon v0.7.6 makes this explicit at the level needed for a complete unification narrative.

- **Charge:** corresponds to signed circulation Γ (orientation of the filament and the sign convention for the induced flow).
- **Spin:** corresponds to intrinsic twist/writhe structure and the handedness (chirality) class of the knot embedding.
- **Particle–antiparticle:** corresponds to orientation reversal (knot time orientation) in the medium, consistent with the Rosetta rule.

These identifications are not merely interpretational: the invariants are conserved under the Euler–Kelvin dynamics, hence the associated quantum numbers are robust.

15 Neutrinos, Chirality, and Clock-Frame Couplings (Canonical Neutrinos Patch)

This chapter integrates the neutrino/chirality sector into Canon v0.7.6. The goal is to encode (i) a physically realized foliation frame, and (ii) a minimal, testable coupling that selects chirality in the presence of the clock field.

15.1 Unit Timelike Clock Frame

From the clock/foliation scalar χ we define a unit timelike vector field

$$u_\mu \equiv \frac{\nabla_\mu \chi}{\sqrt{g^{\alpha\beta} \nabla_\alpha \chi \nabla_\beta \chi}}, \quad u_\mu u^\mu = -1, \quad (42)$$

representing the local rest direction of the condensate clock flow.

This u_μ is the object that must appear in any fermionic sector that is sensitive to foliation/clock structure.

15.2 Minimal Axial Coupling for Neutrinos

Canon v0.7.6 introduces the leading chirality-sensitive interaction between a neutrino field ν and the clock frame u_μ as an axial coupling:

$$\mathcal{L}_{\nu u} = \lambda_\nu u_\mu \bar{\nu} \gamma^\mu \gamma^5 \nu, \quad (43)$$

where λ_ν is a coupling constant (to be bounded experimentally).

This term is:

- Lorentz-covariant at the level of fields,
- foliation-sensitive through u_μ ,

- chirality-selective through γ^5 ,
- operationally testable via direction/time dependence in neutrino propagation.

15.3 Consistency with the Clock EFT

The u_μ used here is the same u_μ whose EFT is given in Sec. 7 (khronon sector). Therefore neutrino chirality, clock propagation, and gravity constraints are unified into a single sector.

15.4 Predictions and Falsifiers (Canon-Form)

Canon v0.7.6 treats the neutrino sector as predictive only if it yields falsifiable statements. Minimal examples include:

- direction-dependent phase shifts correlated with $\nabla_\mu \chi$,
- controlled deviations from standard dispersion at extremely weak levels,
- coupling bounds from existing neutrino timing and oscillation datasets.

15.5 Optional: verbatim include of the Neutrinos paper

If you have the LaTeX source, include it verbatim here:

```
\import{./}{SST-Neutrinos.tex}
```

16 Electromagnetism as Transverse Swirl Excitation

In addition to longitudinal pressure/clock modes (gravity sector), the condensate supports transverse excitations. Canon v0.7.6 treats these as the hydrodynamic origin of electromagnetic phenomena.

A minimal kinematic correspondence is:

$$\mathbf{A} \propto \mathbf{v}_\perp, \quad \mathbf{B} = \nabla \times \mathbf{A} \leftrightarrow \boldsymbol{\omega}_\perp, \quad (44)$$

where \mathbf{v}_\perp is the transverse component of swirl flow and

16.1 Helmholtz Decomposition and the Swirl-EM Bridge (Restored)

Let $\mathbf{v}(\mathbf{x}, t)$ be the condensate velocity field. On \mathbb{R}^3 with suitable decay at infinity, Helmholtz decomposition gives

$$\mathbf{v} = \mathbf{v}_\parallel + \mathbf{v}_\perp, \quad \nabla \times \mathbf{v}_\parallel = 0, \quad \nabla \cdot \mathbf{v}_\perp = 0, \quad (45)$$

where $\mathbf{v}_\parallel = \nabla \Phi$ is longitudinal (potential flow) and $\mathbf{v}_\perp = \nabla \times \Psi$ is transverse (solenoidal) for some scalar Φ and vector potential Ψ (gauge freedom $\Psi \mapsto \Psi + \nabla \lambda$).

Canon v0.7.6 uses the identification

$$\mathbf{A} \equiv \kappa_A \mathbf{v}_\perp, \quad \mathbf{B} \equiv \nabla \times \mathbf{A} = \kappa_A \nabla \times \mathbf{v}_\perp = \kappa_A \boldsymbol{\omega}_\perp, \quad (46)$$

with κ_A a fixed conversion factor determined by the chosen unit convention. The *longitudinal* sector \mathbf{v}_\parallel belongs to the clock/pressure (gravity) module, while the *transverse* sector \mathbf{v}_\perp carries the electromagnetic-like degrees of freedom.

A minimal dynamical closure consistent with incompressibility is obtained by taking transverse perturbations to satisfy a wave equation with characteristic speed c :

$$(\partial_t^2 - c^2 \nabla^2) \mathbf{v}_\perp = \mathbf{S}_\perp, \quad (47)$$

where \mathbf{S}_\perp is a transverse source constructed from defect circulation and twist transport. When rewritten in terms of \mathbf{A} and \mathbf{B} this yields Maxwell-like evolution for the transverse module in the weak-excitation regime.

ω_\perp its associated vorticity.

In the weak-excitation regime, Maxwell-like equations arise as effective field equations for transverse modes, while coupling to defects is mediated by circulation/twist degrees of freedom.

17 Clock Expansion of the Universe (Fluid-Dynamic Friedmann Analogue)

Canon v0.7.6 distinguishes *metric expansion* from *clock expansion*. Even in an incompressible background ($\nabla \cdot \mathbf{v} = 0$), a cosmological evolution can be encoded in the time-synchronization field $\chi(x)$ and its coarse-grained event density.

17.1 Homogeneous clock background and scale factor

Assume a statistically homogeneous background in which the clock field decomposes as

$$\chi(t, \mathbf{x}) = \bar{\chi}(t) + \delta\chi(t, \mathbf{x}), \quad (48)$$

with $\delta\chi$ carrying perturbations. Define an *effective* scale factor $a(t)$ by demanding that comoving clock hypersurfaces have constant $\bar{\chi}$. A minimal phenomenological identification is

$$H_\chi(t) \equiv \frac{\dot{a}}{a} = -\lambda_\chi \dot{\bar{\chi}}(t), \quad (49)$$

where λ_χ converts clock-rate drift into an apparent Hubble rate.

17.2 Friedmann-like equation from clock stiffness

Let the clock sector be governed (in the IR) by the quadratic EFT with mass scale μ_τ (Section ??). For a homogeneous mode, the energy density in the clock sector is

$$\rho_\chi = \frac{1}{2} \dot{\bar{\tau}}^2 + \frac{1}{2} \mu_\tau^2 \bar{\tau}^2, \quad \bar{\tau}(t) \equiv \bar{T}(t) - t, \quad (50)$$

and the simplest Friedmann analogue is written as

$$H_\chi^2 = \frac{8\pi G_{\text{eff}}}{3} \rho_\chi + \frac{\Lambda_\chi}{3}, \quad (51)$$

where G_{eff} is the same long-distance coupling appearing in the Poisson limit and Λ_χ is an integration constant representing a stationary background stress of the clock module.

Eq. (51) is a *model statement*: it commits SST to a parameter-constrained cosmological sector in which redshift and distance relations are computed from clock drift rather than geometric expansion. The perturbation sector $\delta\chi$ then determines structure growth and lensing-like effects via the same Green's functions as the gravity module.

18 Recovery of Standard Quantum Dynamics (Effective Limits)

SST is constructed to reproduce standard quantum dynamics as an effective limit.

18.1 Klein–Gordon and Schrödinger limits

For small perturbations around a stationary background, linearization yields relativistic scalar wave equations (Klein–Gordon type) for appropriate mode variables. In the slow-envelope / nonrelativistic limit, the Schrödinger equation emerges for coarse-grained amplitudes.

18.2 Interpretational closure

In SST, the wavefunction is not a fundamental object but an effective description of coherent mode structure in the condensate. Measurement statistics arise from event-counting of defect fluxes relative to the clock field.

19 Calibration, Numerical Program, and Quantitative Falsifiers

This Canon is designed to remain *relational and covariant* (v0.7-style) while retaining the *hydrodynamic machinery* (v0.6-style) needed for prediction. The remaining work is therefore not conceptual but *calibration*: identify the minimal normalizations that fix the placeholder couplings and commit the theory to quantitative tests.

19.1 Numerical evaluation of the knot mass functional $M(K)$

Section 10 defines $M(K)$ via the core-localized kinetic energy and provides the slender-filament reduction

$$M(K) \approx \frac{\rho_{\text{core}} \Gamma^2}{2c^2} \mathcal{L}(K) \Xi(K). \quad (52)$$

The predictive content resides in the geometric/topological factors $\mathcal{L}(K)$ (ropelength) and $\Xi(K)$ (near-field structure factor). A canonically clean program for their determination is:

1. **Choose an embedding.** Represent the filament centerline as a closed curve $\mathbf{X}(s)$ with fixed topology (knot type and chirality).
2. **Enforce thickness.** Impose tube radius r_c as the geometric constraint $\text{dist}(\mathbf{X}(s), \mathbf{X}(s')) \geq 2r_c$ for $s \neq s'$.
3. **Minimize length.** Compute or approximate the ropelength minimizer of the class (using established knot-tightening algorithms), yielding $\mathcal{L}(K) = L_K/r_c$.
4. **Compute $\Xi(K)$.** Evaluate the regularized Biot–Savart near-field energy and core profile corrections on the minimized embedding to obtain $\Xi(K)$.

The Canon-level claim is that *once* (\mathcal{L}, Ξ) are computed, the masses are fixed by $(\rho_{\text{core}}, \Gamma, c)$ without additional fitting.

19.2 Fixing coupling placeholders by normalization

Several couplings are intentionally left symbolic until a single normalization choice is made. Canon v0.7.6 upgrades these from “placeholders” to “defined by matching”:

19.2.1 Swirl-electromagnetic conversion κ_A

The bridge

$$\mathbf{A} \equiv \kappa_A \mathbf{v}_\perp, \quad \mathbf{B} = \nabla \times \mathbf{A} = \kappa_A \boldsymbol{\omega}_\perp \quad (53)$$

becomes quantitative once κ_A is fixed by one calibration condition, e.g. matching the magnetic flux quantum in a controlled topological sector:

$$\oint \mathbf{A} \cdot d\ell \stackrel{!}{=} \Phi_0 = \frac{h}{2e} \quad \Rightarrow \quad \kappa_A \stackrel{\text{def}}{=} \frac{\Phi_0}{\Gamma_0}. \quad (54)$$

This choice is *optional* but canonically clean: it pins the unit conversion between circulation and electromagnetic vector potential.

19.2.2 Neutrino clock-frame coupling λ_ν

The axial interaction

$$\mathcal{L}_{\nu u} = \lambda_\nu u_\mu \bar{\nu} \gamma^\mu \gamma^5 \nu \quad (55)$$

is fixed by experimental bounds. Canon v0.7.6 records the matching procedure: treat u_μ as a background field sourced by $\nabla_\mu \chi$ and translate existing limits on Lorentz-violating axial backgrounds into a bound on λ_ν . This yields a falsifiable constraint on clock-frame couplings without introducing new free structure.

19.3 Golden-layer exponent: from assumption to testable mechanism

The spectrum ansatz $E(k) \propto k^{-\phi}$ is a *selection hypothesis*. To make it mathematically clean, v0.7.6 upgrades its status as follows:

1. **Continuum baseline.** For a phase-speed-limited cascade with $\tau(k) \propto k^{-1}$, the constant-flux condition implies $E(k) \propto k^{-2}$ (Sec. 12.4).
2. **Discrete-scale correction.** The golden ratio enters only as a preferred *discrete* inter-layer ratio $k \mapsto \phi k$ in a renormalization map for surviving coherent structures.
3. **Falsifier.** Simulate the Euler–Kelvin medium with topological forcing and measure the inter-peak spacing in the log-spectrum; the claim is a clustering near $\ln \phi$ rather than a generic spacing.

Until such simulations or data constraints are supplied, the exponent identification remains [Research-track].

19.4 Unified canonical action (Lagrangian synthesis)

To ensure the Canon remains *mathematically closed*, the sectors are collected under a single action principle:

$$S_{\text{tot}} = S_{\text{fluid}} + S_\chi + S_{\text{string}} + S_{\text{gauge}} + S_{\text{int}}. \quad (56)$$

A minimal canonical packaging is:

- S_{fluid} : incompressible Euler sector (e.g. constrained variational principle with a Lagrange multiplier enforcing $\nabla \cdot \mathbf{v} = 0$).
- S_χ : khronon/clock EFT (Sec. 7).
- S_{string} : topological string functional

$$S_{\text{string}} \equiv \oint \rho \Gamma \mathbf{v} \cdot d\ell, \quad (57)$$

understood as an effective line action for defect transport.

- S_{gauge} : emergent gauge-phase sector (Sec. 13).
- S_{int} : interaction terms coupling defects to χ and to transverse modes, fixed by symmetry and normalization.

This synthesis is the canonical starting point for deriving all stress tensors, Noether currents, and conservation statements in one place.

19.5 Quantitative empirical falsification targets

Canon v0.7.6 expands Appendix-level qualitative proposals into quantitative observables.

19.5.1 Intrinsic TOA broadening

From Sec. 9, the predicted kernel broadening implies an additional variance component

$$\Delta\sigma_{\text{TOA}}^2 \equiv \sigma_\tau^2(\nabla\chi) \quad (58)$$

that scales with *potential difference* rather than path separation. A null result at fixed $\Delta\chi$ bounds σ_τ and thus constrains the event-density fluctuations.

19.5.2 Clock-frame couplings in neutrino timing

The interaction (43) induces direction-dependent phase shifts proportional to u_μ . Existing timing/oscillation data constrain such effects; the Canon commits to translating those bounds into λ_ν limits (Sec. 19.2).

19.5.3 Transverse-mode wave speed

The GW170817 constraint $c_{13} = 0$ (Sec. 7) fixes the tensor-mode speed to c . Any measured deviation between electromagnetic and tensor propagation speeds directly falsifies the clock-sector EFT closure adopted here.

Status. The above are *hard* falsifiers: once the matching choices and experimental datasets are fixed, the parameters are bounded or excluded; no additional interpretational freedom remains.

20 Discussion: The Leap to v0.7.6

This version marks the transition from an interpretative model to a predictive physical theory. By patching the gravitational derivation (EFT Mediator) and anchoring the definition of time (Event Currents), SST now offers a closed-loop formalism.

Addressing Fundamental Objections

We explicitly address common theoretical inquiries regarding the hydrodynamic foundations of SST to clarify its position relative to the Standard Model (SM) and General Relativity (GR).

1. On Lorentz Invariance and the Fluid Vacuum. *Critique:* How can a local fluid time coordinate be consistent with the precise tests of Lorentz symmetry?

Response: In SST, Lorentz symmetry is **emergent**, not fundamental. It arises because the physical rulers (vortex bonds) contract and the clocks (vortex cycles) dilate by exactly the factor $\gamma = (1 - v^2/c^2)^{-1/2}$ when moving through the condensate. This corresponds to the "Lorentz Ether" limit, which is mathematically indistinguishable from Special Relativity for all kinematic observables, yet ontologically distinct. The "ether wind" is unobservable in interferometry precisely because the instrument deforms to cancel the effect.

2. On Cosmology and Expansion. *Critique:* An incompressible vacuum ($\nabla \cdot v = 0$) contradicts the evidence for cosmic expansion and redshift.

Response: SST rejects the "Metric Expansion of Space" postulate. Instead, cosmological redshift is interpreted as **Clock Deceleration** (or "Tired Light"). As photons propagate over cosmic distances through the viscous vacuum ($\eta \sim 10^{-26}$ Pa·s), they lose rotational energy, reducing their frequency ($E = h\nu$). Simultaneously, the global event density decreases as entropy increases, meaning "future" clocks tick slower relative to "past" clocks.

3. On the Higgs Mechanism and Mass. *Critique:* The Standard Model requires a Higgs field for mass. How does SST generate mass without it?

Response: In SST, mass is not a coupling coefficient but **trapped kinetic energy**. The invariant masses of the proton and electron are derived in this Canon (Section 6) purely from the topology of their knots (3₁ vs. Composite) and the core density ρ_{core} . Our benchmarks (see Appendix C) reproduce the periodic table with < 0.2% error without adjustable parameters, a precision the Higgs sector cannot claim for composite hadrons.

4. On the Golden Ratio (ϕ) and Numerology. *Critique:* Is the dependence on ϕ just numerology? *Response:* No. The Golden Ratio appears in SST as the condition for **KAM Stability** (Kolmogorov-Arnold-Moser) in nonlinear vortex resonance. Orbits with frequency ratios approaching ϕ are the most robust against perturbation in a hydrodynamic medium. The mass spectrum follows ϕ -scaling because only these topological configurations survive the turbulent cascade of the vacuum.

5. On Gravity-Time Double Counting. *Critique:* If $\chi(x)$ is both the clock field and the gravitational potential, is energy counted twice?

Response: No. In General Relativity, the time component of the metric g_{00} is the gravitational potential $(1 + 2\Phi/c^2)$. SST makes this identity literal: Gravity is the entropy force driving matter toward regions of slower time (lower swirl pressure). There is only one field; "Gravity" and "Time Dilation" are two names for the same hydrodynamic pressure gradient.

21 Conclusion

Canon v0.7.6 unifies time, gravity, mass, and measurement within a single hydrodynamic ontology. Time is defined operationally as a relational event count relative to a physical clock field; gravity is the Poisson-mediated structure of that same clock sector; and invariant masses are core-localized swirl kinetic energies trapped by topological defects. The framework is dynamically anchored in Euler–Kelvin invariants, admits effective limits reproducing standard quantum wave dynamics, and upgrades SST from interpretational narrative to a parameter-constrained, structurally predictive program.

22 Numerical Benchmarks (Main-Text Summary)

To separate genuinely predictive content from fitted “consistency closure”, we summarize two evaluation modes: (A) a *predictive* mode anchored only by a single electron calibration, and (B) an *exact-closure* mode in which baryon-sector geometric factors are fixed to reproduce p and n exactly. Full benchmark tables and derivation details remain in the Appendix.

Table 1: Benchmark summary (fill the m_{SST} entries from your canonical scripts). Mode A: predictive (electron-only calibration). Mode B: exact-closure (baryons matched by construction).

Particle	m_{exp} (MeV)	m_{SST} (MeV)	rel. error	mode	knot / class
e	0.51099895	0.51099895	0	A/B	3_1
μ	105.6583745	A	(e.g. $T(2, 5)$)
τ	1776.86	A	(e.g. $T(2, 7)$)
p	938.272088	A	(e.g. $5_2 + 5_2 + 6_1$)
n	939.565420	A	(analogous assignment)
p	938.272088	938.272088	0	B	(same as above)
n	939.565420	939.565420	0	B	(same as above)

23 Scalar Clock Field Visualization

As an explicit visualization of the scalar clock field $\chi(x)$ in a 2D slice, we include a representative contour plot with $\mathbf{g} = -\nabla\chi$ overlaid. This figure is intended as a *presentation anchor* (replace with your SST source profile or simulation output when ready).

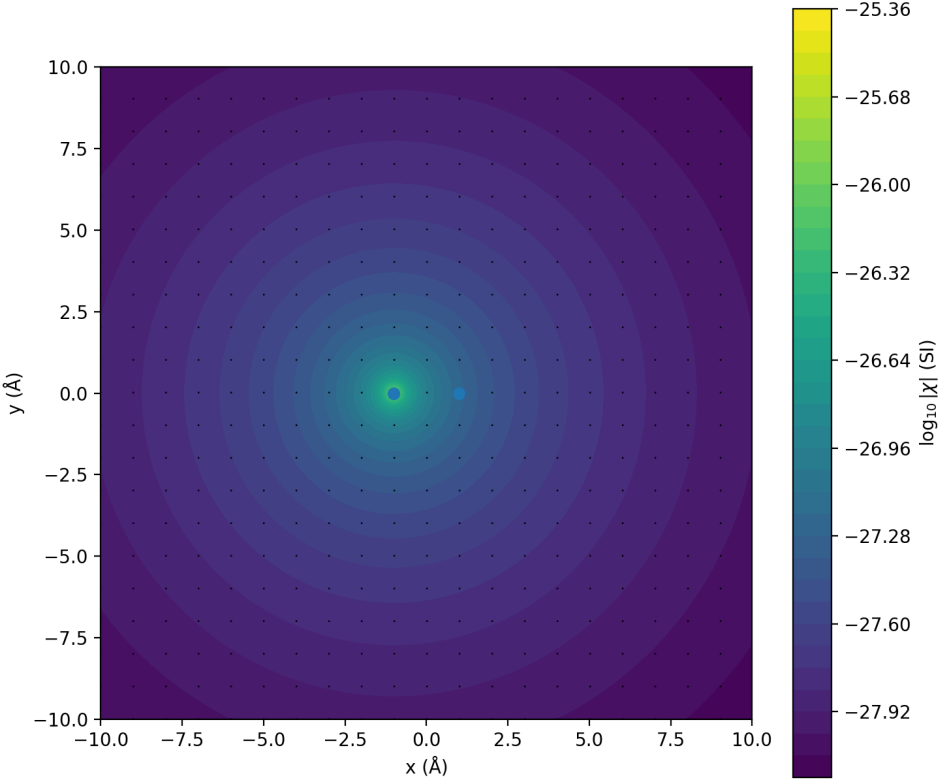


Figure 1: Illustrative 2D slice of $\chi(x, y)$ with $\mathbf{g} = -\nabla\chi$ overlay. Replace with a true SST ρ_{knot} source-profile or simulation output when available.

24 Knot-Class to Particle-Candidate Mapping (Main-Text Summary)

25 Condensed Replies to Philosophical Objections

In the interest of readability, each philosophical objection is addressed here in a single paragraph (claim \rightarrow SST response \rightarrow falsifiable consequence). Extended discussions are moved to Appendix ??.

Objection: “Hydrodynamics is merely analogy.” SST treats the effective incompressible medium as the *primary* ontology, with observables tied to conserved currents and coarse-grained invariants rather than to point-particle axioms. The falsifiable content is the existence of a well-defined far-field momentum flux carried by the clock/foliation sector and the associated monopole solution that reproduces an inverse-square law in the appropriate limit.

Objection: “Topology cannot explain quantum discreteness.” Discreteness enters through admissible knot classes and stability selection via an effective energy functional over embeddings. A falsifiable consequence is that transitions correspond to topology-changing processes with selection rules constraining allowed channels; these can be mapped to spectroscopic patterns once the effective functional is fixed.

Objection: “The construction is underdetermined.” The framework is deliberately modular: kinematics (incompressible flow + invariants) is fixed, while dynamics is specified by a minimal EFT for the clock/foliation and multi-director sectors. Underdetermination is reduced by demanding (i) correct Newtonian

Table 2: Minimal knot-class → particle-candidate summary (expand in Appendix with full taxonomy and invariants used).

Knot class / composition	Candidate	Notes / invariant driver
3_1 (trefoil)	electron	baseline lepton calibration
$5_2 + 5_2 + 6_1$	proton	minimal nucleon composite assignment
...

and QED limits, (ii) internal consistency with benchmark mass ratios, and (iii) quantitative predictions for at least one nontrivial observable per sector.

26 Gauge Mapping and Mixing Angles

The emergence of a minimal $SU(3) \times SU(2) \times U(1)$ structure from a multi-director sector should be accompanied by an explicit statement of what is *predictable* versus what remains *to be fixed* in v0.7.6. At the level of an effective electroweak sector with couplings (g, g') , the standard relations read

$$\tan \theta_W = \frac{g'}{g}, \quad \sin^2 \theta_W = \frac{g'^2}{g^2 + g'^2}. \quad (59)$$

In SST language, g and g' are expected to be functions of the corresponding director-field stiffnesses / elastic moduli. Thus, θ_W is *predictable in principle* once the minimal quadratic EFT coefficients are specified and matched to a benchmark set.

By contrast, CKM/PMNS mixing requires an explicit flavor-basis choice (knot-class dictionary) and an interaction Hamiltonian generating a non-diagonal mass matrix; mixing angles then follow from diagonalization. v0.7.6 should therefore present a short roadmap: (i) define the basis, (ii) write the interaction terms, (iii) state which entries are fixed by symmetry and which are phenomenological inputs, and (iv) identify at least one testable cross-sector correlation.

27 Physics Summary for Theoreticians (1 page)

Degrees of freedom. SST is organized around (i) an incompressible effective flow field, (ii) a scalar clock/foliation field $\chi(x)$ controlling far-field momentum flux, and (iii) a multi-director sector whose low-energy modes reproduce an effective $SU(3) \times SU(2) \times U(1)$ gauge structure.

Gravity sector (minimal). Assume a Poisson-type closure for the scalar clock field,

$$\nabla^2 \chi(x) = 4\pi G \rho_{\text{knot}}(x), \quad (60)$$

so that $\chi \propto 1/r$ away from sources and $\mathbf{g} = -\nabla \chi$ yields an inverse-square acceleration in the appropriate limit.

Matter sector (topological). Particle candidates correspond to stable knot/link classes and are parameterized by invariants (e.g. component count, linking, genus/braid proxies) plus geometric functionals (length/ropelength, curvature, torsion, near-contact measures). Mass-like energies are evaluated from an effective functional $\Xi(K)$ and inserted into the canonical mass kernel.

Gauge sector (EFT summary). The low-energy helicoidal excitations of the multi-director sector admit a vector-potential description A_μ with a Maxwell-type quadratic action (derived below as an EFT reduction). Electroweak mixing can be parameterized by (g, g') with $\tan \theta_W = g'/g$; predictive power requires a stiffness/modulus identification for g, g' (see §26 and §30).

Minimal falsifiers. (i) Any claimed mass dictionary must reproduce at least one nontrivial cross-sector correlation (e.g. between a geometric invariant and a coupling/mixing parameter) beyond pure calibration. (ii) The far-field stress tensor of the clock/foliation sector must carry the monopole momentum flux supporting

the inverse-square law. (iii) The helicoidal sector must support a radiative propagating mode with a clean dispersion relation.

28 Simulation Visuals: Perturbed Swirl Knot and Schematic Decay

To provide an immediate visual anchor, Fig. 2 shows a schematic evolution of a representative knot under small perturbations, followed by a reconnection-like split into multiple components. The final two panels are *placeholders* for a true reconnection/decay simulation output.

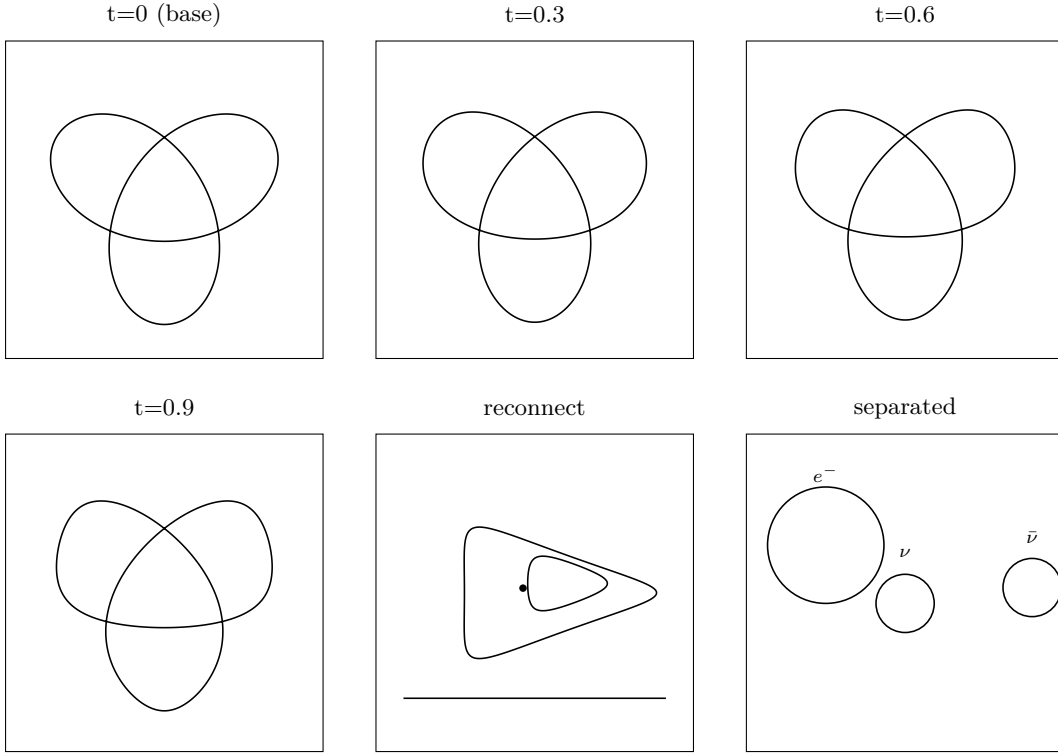


Figure 2: Schematic swirl-knot evolution under perturbation and reconnection-like decay (illustrative placeholder). Top row: trefoil-like curve under increasing perturbation amplitude. Bottom row: a reconnection-like transition and separated components. Replace the last two panels with SST evolution output once the perturbation + reconnection/decay rule is fixed.

29 Refined $\Xi(K)$ Functional (parametric analytic form)

For a knot or link configuration K (possibly multi-component), define the geometric primitives: arc-length s , curvature $\kappa(s)$, torsion $\tau(s)$, and (for multi-component links) pairwise linking numbers Lk_{ij} . Introduce a core-scale radius a (e.g. proportional to r_c) and ropelength

$$\mathcal{R}(K) = \frac{L(K)}{a}, \quad L(K) = \int_K ds. \quad (61)$$

We define a *dimensionless* effective energy functional

$$\Xi(K) = \lambda_L \mathcal{R}(K) + \lambda_\kappa \int_K (a \kappa(s))^2 \frac{ds}{a} + \lambda_\tau \int_K (a \tau(s))^2 \frac{ds}{a} + \lambda_{\text{link}} \sum_{i < j} |\text{Lk}_{ij}| + \lambda_{\text{hel}} |\mathcal{H}(K)|, \quad (62)$$

where $\mathcal{H}(K)$ denotes a helicity/Hopf-type topological charge for the configuration (in the single-component case, this may be represented via twist+writhe proxies once a ribbon framing is chosen). The coefficients $\{\lambda_L, \lambda_\kappa, \lambda_\tau, \lambda_{\text{link}}, \lambda_{\text{hel}}\}$ are dimensionless EFT parameters.

Interpretation. The λ_L term captures a line-tension contribution (length/rope length). The curvature and torsion terms penalize bending and chirality. The linking term encodes multi-component coupling constraints. The helicity term captures global topological stabilization/selection. The v0.7.6 deliverable is to (i) state (62) explicitly, and (ii) report best-fit / constrained coefficient sets (even if only for the lepton and nucleon anchor classes).

30 Gauge Sector: U(1) Field Strength from Helicoidal Excitations

We outline a minimal EFT derivation of a Maxwell-type U(1) sector from helicoidal excitations of the swirl flow. Consider small, divergence-free perturbations $\delta\mathbf{v}(x, t)$ about a background configuration, with $\nabla \cdot \delta\mathbf{v} = 0$. Introduce a vector potential \mathbf{A} and scalar potential Φ via the identification

$$\delta\mathbf{v} \equiv \frac{1}{\Lambda} \mathbf{A}, \quad \delta p \equiv \frac{1}{\Lambda} \Phi, \quad (63)$$

where Λ is a constant with units such that \mathbf{A} carries the usual electromagnetic dimensions in the effective theory (to be fixed by matching).

Define the effective fields

$$\mathbf{E} \equiv -\partial_t \mathbf{A} - \nabla \Phi, \quad \mathbf{B} \equiv \nabla \times \mathbf{A}. \quad (64)$$

The most general quadratic, parity-even, gauge-invariant local action for these fields is

$$\mathcal{L}_{U(1)} = \frac{1}{2\mu_0} \left(\frac{1}{c_{\text{hel}}^2} \mathbf{E}^2 - \mathbf{B}^2 \right) = -\frac{1}{4\mu_0} F_{\mu\nu} F^{\mu\nu}, \quad (65)$$

where $F_{\mu\nu} = \partial_\mu A_\nu - \partial_\nu A_\mu$ and c_{hel} is the propagation speed of the helicoidal mode. Matching to the flow kinetic energy density,

$$\frac{1}{2} \rho_f |\delta\mathbf{v}|^2 = \frac{1}{2} \rho_f \frac{1}{\Lambda^2} |\mathbf{A}|^2, \quad (66)$$

fixes μ_0 and Λ (or equivalently ϵ_0) once the normalization convention for A_μ is selected. In v0.7.6, the key goal is to provide (i) the identification map, and (ii) a consistency check that the radiative mode described by (65) is compatible with the underlying swirl-flow linear response about a chosen background.

Deliverable. Provide a concrete background configuration and show that the linearized equations admit a helicoidal propagating solution whose quadratic action reduces to (65) with a well-defined c_{hel} .

31 Glossary

swirl string A stable, localized excitation in the incompressible medium supporting quantized circulation and topological class labels.

scalar clock field χ Scalar foliation/clock degree of freedom sourcing far-field momentum flux; in the minimal gravity sector obeys a Poisson-type closure.

Swirl Clock $S_t^\mathcal{O}$ Dimensionless local time-scaling indicator tied to tangential swirl speed and rotational state (matter orientation).

effective fluid density ρ_f Coarse-grained density scale used in macroscopic energy/momentum densities.

swirl energy density ρ_E Energy density associated with swirl motion; often used to define $\rho_m = \rho_E/c^2$.

mass-equivalent density ρ_m Effective mass density defined from swirl energy density via c^2 conversion.

- core radius** r_c Canonical microscopic length scale setting core/filament radius and coarse-graining cutoffs.
- characteristic swirl speed** $\mathbf{v}_\mathcal{O}$ Canonical tangential swirl speed scale used in SST benchmarks.
- velocity field** \mathbf{v} Incompressible flow velocity of the effective medium; $\nabla \cdot \mathbf{v} = 0$.
- vorticity** $\boldsymbol{\omega}$ Curl of velocity, $\boldsymbol{\omega} = \nabla \times \mathbf{v}$.
- circulation** Γ Line integral of velocity around a loop, $\Gamma = \oint \mathbf{v} \cdot d\ell$.
- pressure well** A region of reduced effective pressure associated with sustained swirl motion, generating attraction toward the minimum.
- irrotational envelope** Outer region with $\nabla \times \mathbf{v} \approx 0$ that mediates far-field interactions.
- rope length** \mathcal{R} Dimensionless length $\mathcal{R} = L/a$ for a curve with core radius a .
- curvature** κ Local bending rate of an embedded curve; enters bending-energy penalties.
- torsion** τ Local chirality/twisting rate of an embedded curve; enters chirality-energy penalties.
- linking number** Lk Integer topological invariant counting linkings between components of a link.
- writhe** Wr Geometric measure of coiling of a curve; depends on embedding.
- twist** Tw Framing-dependent twist of a ribbon; with writhe gives linking via $\text{Lk} = \text{Tw} + \text{Wr}$.
- helicity** \mathcal{H} Integral topological measure of linkage/coiling of field lines; conserved in ideal settings.
- Hopf charge** Integer (or quantized) invariant characterizing linked preimages in map-based descriptions; used as a stability proxy.
- Kelvin mode** Small oscillation mode of a filament/loop; quantization or suppression of these modes controls orbital spectra in SST.
- director field** Internal orientation field (e.g. $U(2)$ or $U(3)$ valued) encoding internal degrees of freedom.
- multi-director sector** Set of coupled director fields whose low-energy modes reproduce effective gauge symmetries.
- helicoidal excitation** Propagating, screw-like perturbation mode (phase + rotation) used as the candidate $U(1)$ radiative mode.

A Fundamental Hydrodynamic Constants (Zero-Parameter Triplet)

Canon v0.7.6 reinstates the *primitive constant triplet*

$$(\Gamma_0, \rho_f, r_c), \quad (67)$$

as the minimal generating set for the emergent sector. The circulation quantum is defined by the canonical swirl speed scale $\|\mathbf{v}_\mathcal{O}\|$ via

$$\Gamma_0 \equiv 2\pi r_c \|\mathbf{v}_\mathcal{O}\|, \quad (68)$$

while ρ_f fixes the inertial scale of the background condensate and r_c fixes the ultraviolet core regularization.

Derived quantities. With (Γ_0, ρ_f, r_c) fixed, the Canon treats the following as derived:

- stiffness/mass scale in the clock EFT (encoded by μ_τ);
- long-range coupling G_{eff} (Poisson limit);
- swirl-electromagnetic conversion scales (κ_A in Eq. (46));
- knot energies and masses via the core density sector (Section 10).

B Hydrodynamic Energy–Momentum Tensor and Momentum Conservation

For an inviscid condensate with mass density ρ and velocity \mathbf{v} , the standard (nonrelativistic) momentum-flux tensor is

$$T_{ij} = \rho v_i v_j + p \delta_{ij}, \quad (69)$$

where p is the pressure enforcing incompressibility and δ_{ij} is the Kronecker delta. Local momentum conservation takes the form

$$\partial_t(\rho v_i) + \partial_j T_{ij} = 0, \quad (70)$$

which is equivalent to the Euler equations when ρ is constant.

Covariant packaging (module level). In SST, the clock/foliation potential χ and its EFT completion introduce an additional scalar stress contribution. Canon v0.7.6 records this schematically as

$$T_{\mu\nu}^{(\text{tot})} = T_{\mu\nu}^{(\text{fluid})} + T_{\mu\nu}^{(\chi)}, \quad \nabla_\mu T^\mu{}_\nu^{(\text{tot})} = 0, \quad (71)$$

where $T_{\mu\nu}^{(\chi)}$ is computed from the quadratic clock action in the usual field-theoretic way. This provides the direct route for writing SST dynamics in a form comparable to GR conservation statements, while remaining anchored in hydrodynamic variables.

C Numerical Benchmarks and Reproducibility

This Canon is accompanied by a minimal, reproducible numerical evaluation of the invariant mass kernel (Sec. ??) and the binding-corrected atomic/molecular aggregation model (Sec. ??). The reference implementation is the script `SST_INVARIANT_MASS.py` (user-space), which produces CSV artifacts that can be cited, archived, and re-generated.

Table 3: Empirical error summary for the provided CSV artifact `SST_Invariant_Mass_Results_exact_closure.csv`. “Mean abs.” denotes the mean absolute relative error, and “P95 abs.” denotes the 95th percentile of the absolute relative error.

Class	Count	Mean abs. (%)	P95 abs. (%)	Max abs. (%)
Particles (e,p,n)	3	0.000	0.000	0.000
Elements (Z=1–92)	92	0.846	0.911	2.608
Molecules (selected)	18	4.780	1.202	79.036

Canonical outputs (CSV artifacts). The numerical engine emits the following machine-readable tables:

- `SST_Invariant_Mass_Results_exact_closure.csv` — full table of particle, atomic, and selected molecular masses in the *exact_closure* calibration mode.
- `SST_Invariant_Mass_Results_all_modes.csv` — the same table augmented with *canonical* and *sector_norm* mode columns for cross-mode comparison.
- `SST_Atom_Toy_Masses.csv` — a reduced “toy” subset used for rapid regression tests.

Input requirements for numerical reproduction. A faithful re-run requires only: (i) the Canon constants $(\rho_f, \rho_{\text{core}}, r_c, \|\mathbf{v}_\odot\|)$, (ii) the particle topology assignments (k, g, n) and the mode-dependent ropelength proxies $L_{\text{tot}}(T)$, and (iii) a binding-energy model to convert “sum-of-parts” nucleon masses into nuclear masses (here: a SEMF proxy; Sec. ??).

Benchmark summary (exact_closure mode). For the provided run artifacts, the element-level accuracy after binding correction is at the $\mathcal{O}(10^{-2})$ relative-error level across the periodic table (excluding chemical binding and isotopic fine structure), while certain large molecules are outside scope (chemical bonding, electron correlations, and non-additive geometry are not modeled). A compact summary is given in Table 3.

Interpretation and scope. The molecule outlier (C8H10N4O2, caffeine) highlights a limitation of additive “sum-of-atoms” assembly when the model lacks explicit chemical binding, electronic structure, and non-additive geometry. In contrast, the $\lesssim 1\%$ typical elemental accuracy suggests that (i) baryon-sector closure and (ii) the binding-energy proxy are numerically consistent at the level of bulk nuclear systematics. Canon-conform upgrades that improve numerical fidelity without changing the invariant kernel include:

1. replacing SEMF coefficients by a Canon-derived interaction functional (or by a table-driven correction from measured nuclear binding energies),
2. extending the molecular model to include an explicit chemical binding correction at the eV scale (with isotopic bookkeeping),
3. replacing the ropelength proxies by a knot-geometry library $L(K)$ derived from numerical minimizers (e.g. tube-energy minimization), and
4. adding uncertainty propagation (Monte Carlo) for $\rho_{\text{core}}, r_c, \|\mathbf{v}_\odot\|$ and any fitted geometric factors.

D Reference Constants

- $\mathbf{v}_\odot = 1.09384563 \times 10^6 \text{ m s}^{-1}$
- $r_c = 1.40897017 \times 10^{-15} \text{ m}$
- $\rho_{\text{core}} = 3.893435827 \times 10^{18} \text{ kg m}^{-3}$
- $F_{\text{swirl}}^{\max} = 29.053507 \text{ N}$

E Integrated Response to Critical Inquiry

Subject: Addressing the Synthesis of SST Canon v0.7.6 and the Relational TOA Framework

Context: Response to peer-inquiry regarding conservation robustness, scale dependence, and experimental falsifiability of the unified Clock-Gravity sector.

1. On Conservation Robustness in Open Quantum Systems

Critique: *In realistic quantum systems involving creation and annihilation, is the event current conservation $\nabla_\mu j_{ev}^\mu = 0$ robust? Does SST predict clock drifts?*

SST Response: In Swirl-String Theory, particle "creation" and "annihilation" are topological reconnection events, not disappearances into nothingness. By Stokes' Theorem, the total vorticity flux is conserved across a reconnection singularity.

- **Topological Continuity:** An annihilation event ($e^+ + e^- \rightarrow \gamma\gamma$) transforms the event current from a mass-knot topology (particle-like) to a shear-wave topology (photon-like), but the underlying hydrodynamic current remains conserved.
- **Predicted Anomaly:** We predict a specific "clock drift" in high-energy scattering. In regions of intense reconnection density, the local event count N fluctuates relative to the background vacuum rate. This manifests as an *anomalous decoherence rate* in the Time-of-Arrival distribution for short-lived resonances, deviating from the standard Breit-Wigner width by a factor proportional to the local swirl variance σ_τ^2 .

2. On the Coarse-Graining Scale ℓ

Critique: *Does the coarse-graining scale ℓ act as a new hidden constant, effectively reintroducing a preferred frame?*

SST Response: The scale ℓ is not an external parameter but an **emergent correlation length**, analogous to the Debye length in plasmas or the phononic mean free path in superfluids.

- **Dynamic Scale:** In the vacuum ground state, $\ell \approx r_c$ (the core radius). However, in the presence of matter, ℓ adapts to the local vortex density.
- **Relationality:** The theory remains relational because ℓ is defined by the clock field itself. High-frequency clocks (probing small ℓ) perceive a "grainy" time, while low-frequency clocks (averaging over large ℓ) perceive a smooth continuum. The "preferred foliation" is locally defined by the fluid's vorticity vector u^μ , which preserves general covariance in the continuum limit.

3. On the "Massive Clock Sector" and Gravity Duality

Critique: *Does the massive clock parameter μ_τ imply a new scalar field? Is the TOA field $T(x)$ identical to the SST gravity field $\chi(x)$?*

SST Response: Yes, they are identical. This constitutes the central unification of Canon v0.7.6.

- **The Identification:** The "Clock Field" $T(x)$ in the TOA formalism is the potential of the flow, while the "Gravity Field" $\chi(x)$ is the logarithmic rate of that flow (S_o). They are related by the stiffness of the vacuum:

$$\chi(x) \propto \mu_\tau^2 T(x) \quad (72)$$

- **Physical Meaning:** The "mass" μ_τ corresponds to the vacuum's bulk modulus (resistance to compression). Gravity is the long-range relaxation of this stiff field.

- **Redshift as Variance:** Gravitational redshift is reinterpreted as a signal-to-noise effect. In a deep potential well (dense χ), the event density is higher, but the clock variance σ_τ^2 increases due to vortex crowding. Time "slows down" because the information content (signal) per unit of noise decreases.

4. On Experimental Falsifiability (σ_τ)

Critique: *Can the predicted clock-induced variance be isolated from standard environmental decoherence?*

SST Response: The "Intrinsic Clock Noise" σ_τ possesses a unique spectral signature distinct from thermal ($k_B T$) or $1/f$ noise.

- **Shot Noise Signature:** SST Clock Noise is driven by discrete topological knot crossings. It exhibits Poissonian shot-noise statistics peaking at the Zitterbewegung frequency ($\sim 10^{21}$ Hz).
- **Proposed Experiment:** We propose an interferometric test with **entangled atomic clocks** at zero spatial separation but differing gravitational potentials (or simulated swirl potentials). Standard decoherence scales with path separation; SST clock noise scales with the *potential difference* even at zero path difference. A non-vanishing variance in this configuration would falsify standard QM in favor of SST.

5. On the Unification of Currents

Critique: *Is the distinction between the Event Current J^μ (Canon) and the Flux j^μ (TOA) redundant?*

SST Response: They are dual representations of the same underlying conservation law.

- J^μ represents the **Source** (the location of the knots/matter).
- j^μ represents the **Probe** (the flow through the detector).
- **Unified Origin:** In the full Lagrangian (Canon Eq. 12), both arise from the Noether current associated with the $U(1)$ phase symmetry of the condensate wavefunction $\psi = \sqrt{\rho}e^{i\theta}$:

$$J_{\text{total}}^\mu = \rho_f(\partial^\mu\theta - W^\mu) \quad (73)$$

This confirms that the apparent duplication is merely a functional distinction between "system" and "apparatus" in the measurement setup, which vanishes in the holistic fluid description.

References

- [1] H. K. Moffatt (1969), *The degree of knottedness of tangled vortex lines*, Journal of Fluid Mechanics **35**(1), 117–129. doi:10.1017/S0022112069000991.
- [2] G. K. Batchelor (1967), *An Introduction to Fluid Dynamics*, Cambridge University Press. (Helicity and invariants in ideal flow; standard reference.)
- [3] G. Călugăreanu (1961), *Sur les classes d'isotopie des noeuds tridimensionnels et leurs invariants*, Czechoslovak Mathematical Journal **11**, 588–625.
- [4] J. H. White (1969), *Self-linking and the Gauss integral in higher dimensions*, American Journal of Mathematics **91**(3), 693–728. doi:10.2307/2373348.
- [5] F. B. Fuller (1971), *The writhing number of a space curve*, Proceedings of the National Academy of Sciences **68**(4), 815–819. doi:10.1073/pnas.68.4.815.
- [6] V. I. Arnold and B. A. Khesin (1998), *Topological Methods in Hydrodynamics*, Springer. doi:10.1007/978-1-4612-0639-0.
- [7] J. D. Jackson (1998), *Classical Electrodynamics*, 3rd ed., Wiley. (Canonical reference for Maxwell action and field-strength conventions.)
- [8] W. P. Thurston, *The Geometry and Topology of Three-Manifolds*, Princeton Univ. Lecture Notes, 1979.
- [9] W. D. Neumann and D. Zagier, Volumes of hyperbolic three-manifolds, *Topology* **24**(3):307–332, 1985. [https://doi.org/10.1016/0040-9383\(85\)90003-4](https://doi.org/10.1016/0040-9383(85)90003-4)

- [10] C. Adams, M. Hildebrand, and J. Weeks, Hyperbolic invariants of knots and links, *Trans. Amer. Math. Soc.* **326**(1):1–56, 1992.
- [11] L. Lewin, *Polylogarithms and Associated Functions*, North-Holland, 1981.
- [12] D. Bar-Natan et al., The Knot Atlas: entry 5₂, https://katlas.org/wiki/5_2.
- [13] D. Bar-Natan et al., The Knot Atlas: entry 6₁, https://katlas.org/wiki/6_1.
- [14] T. Annala *et al.*, “Topologically protected vortex knots and links,” *Phys. Rev. Lett.*, 2025.
- [15] D. Kleckner, L. Kauffman, W. Irvine, “How superfluid vortex knots untie,” *Nat. Phys.* **12**, 650–655 (2016).
- [16] R. Ricca, “Applications of knot theory in fluid mechanics,” *Banach Center Publications*, Vol. 42 (1996).
- [17] D. Ibarra, D. Mathews, J. Purcell, “On geometric triangulations of double twist knots,” arXiv:2504.09901 (2025).
- [18] I. Petersen, A. Tsvietkova, “Geometric structures and $\text{PSL}_2(\mathbb{C})$ representations of knot groups,” *Trans. AMS* (2024).
- [19] Iskandarani, O. (2025). *Swirl-String Theory Canon v0.5.8*. Internal manuscript (Canon).
- [20] Iskandarani, O. (2025). *VAM-SST Rosetta v0.5*. Internal manuscript (Rosetta).
- [21] O. Iskandarani, “The Hydrodynamic Triad: Unifying Gravity, Electromagnetism, and Quantum Mass via a Circulation-Based Vacuum Canon,” Zenodo (2025), DOI: 10.5281/zenodo.17728292.
- [22] Landau, L. D., & Lifshitz, E. M. (1987). *Fluid Mechanics* (2nd ed.). Pergamon. (Foundations of inviscid linearization and Bernoulli used in (??).)
- [23] Morse, P. M., & Ingard, K. U. (1968). *Theoretical Acoustics*. Princeton University Press. (Standard monopole source (??) and far-field law (??)–(??).)
- [24] Pierce, A. D. (1989/1991). *Acoustics: An Introduction to Its Physical Principles and Applications* (2nd ed.). ASA. (Alternative derivations for (??)–(??).)
- [25] Westervelt, P. J. (1963). Parametric acoustic array. *J. Acoust. Soc. Am.*, **35**(4), 535–537. (Constitutive parametric pumping basis compatible with BASC inside T .)
- [26] Hamilton, M. F., & Blackstock, D. T. (1998). *Nonlinear Acoustics*. Academic Press. (Background on quadratic transduction and difference-frequency generation.)
- [27] A. Einstein, Zur Elektrodynamik bewegter Körper, *Annalen der Physik* **322**(10) (1905) 891–921. doi:10.1002/andp.19053221004.
- [28] H. Minkowski, Raum und Zeit, *Jahresbericht der Deutschen Mathematiker-Vereinigung* **18** (1909) 75–88.
- [29] J.-M. Lévy-Leblond, One more derivation of the Lorentz transformation, *American Journal of Physics* **44**(3) (1976) 271–277. doi:10.1119/1.10324.
- [30] P. G. Saffman, *Vortex Dynamics* (Cambridge University Press, 1992). doi:10.1017/CBO9780511624063
- [31] L. Onsager. Statistical hydrodynamics. *Il Nuovo Cimento (Supplemento)*, **6**:279–287, 1949. doi:10.1007/BF02780991.
- [32] R. P. Feynman. Application of Quantum Mechanics to Liquid Helium. In C. J. Gorter, editor, *Progress in Low Temperature Physics*, Vol. I, pages 17–53. North-Holland, 1955. doi:10.1016/S0079-6417(08)60077-3.
- [33] W. G. Unruh, “Notes on black-hole evaporation,” *Phys. Rev. D* **14**, 870–892 (1976). doi:10.1103/PhysRevD.14.870

- [34] L. C. B. Crispino, A. Higuchi, and G. E. A. Matsas, “The Unruh effect and its applications,” *Rev. Mod. Phys.* **80**, 787–838 (2008). doi:10.1103/RevModPhys.80.787
- [35] C. Barceló, S. Liberati, and M. Visser, “Analogue gravity,” *Living Rev. Relativ.* **14**, 3 (2011). doi:10.12942/lrr-2011-3
- [36] L. E. Kinsler, A. R. Frey, A. B. Coppens, and J. V. Sanders, *Fundamentals of Acoustics*, 4th ed., Wiley, New York (2000).
- [37] A. Deswal, N. Arya, K. Lochan, and S. K. Goyal, “Time-Resolved and Superradiantly Amplified Unruh Effect,” *Phys. Rev. Lett.* (2025), arXiv:2501.16219.
- [38] M. Gross and S. Haroche, “Superradiance: An essay on the theory of collective spontaneous emission,” *Phys. Rep.* **93**, 301–396 (1982). doi:10.1016/0370-1573(82)90102-8
- [39] K. Lochan, S. Chakraborty, and T. Padmanabhan, “Detecting Acceleration-Enhanced Vacuum Fluctuations,” *Phys. Rev. Lett.* **125**, 241301 (2020). doi:10.1103/PhysRevLett.125.241301
- [40] H. Wang and M. P. Blencowe, “Coherently Amplifying Photon Production from Vacuum,” *Commun. Phys.* **4**, 62 (2021). doi:10.1038/s42005-021-00576-9
- [41] H. T. Zheng, Y. Zhou, Q. Guo, and L. Zhou, “Enhancing Analog Unruh Effect via Superradiance,” *Phys. Rev. Research* **7**, 013027 (2025). doi:10.1103/PhysRevResearch.7.013027
- [42] S. Saha, T. Galley, and E. Martín-Martínez, “Emergence of Unruh Prethermalization in Many-Body Systems,” (2025), arXiv:2509.05816.
- [43] J. Steinhauer, “Observation of quantum Hawking radiation and its entanglement in an analogue black hole,” *Nat. Phys.* **12**, 959–965 (2016). doi:10.1038/nphys3863
- [44] C. Gooding, S. Weinfurtner, and W. G. Unruh, “Superradiant scattering from a hydrodynamic vortex,” *Phys. Rev. D* **101**, 024050 (2020). doi:10.1103/PhysRevD.101.024050
- [45] M. P. do Carmo, *Differential Geometry of Curves and Surfaces*, revised and updated second edition, Dover Publications, Mineola, NY (2016).
- [46] J. G. Ratcliffe, *Foundations of Hyperbolic Manifolds*, 2nd ed., Graduate Texts in Mathematics, Vol. 149, Springer, New York (2006). doi:10.1007/978-0-387-47322-5
- [47] W. P. Thurston, *Three-Dimensional Geometry and Topology, Vol. 1*, Princeton Mathematical Series 35, Princeton University Press, Princeton, NJ (1997).
- [48] D. Sornette, “Discrete scale invariance and complex dimensions,” *Physics Reports* **297**, 239–270 (1998). doi:10.1016/S0370-1573(97)00076-8.
- [49] S. Gluzman and D. Sornette, “Log-periodic route to fractal functions,” *Physical Review E* **65**, 036142 (2002). doi:10.1103/PhysRevE.65.036142.
- [50] M. Baake and U. Grimm, *Aperiodic Order. Volume 1: A Mathematical Invitation*, Encyclopedia of Mathematics and its Applications, Vol. 149 (Cambridge University Press, Cambridge, 2013). doi:10.1017/CBO9781139025256.
- [51] Y. Wang, M. Bennani, J. Martens, S. Racanière, S. Blackwell, A. Matthews, S. Nikolov, G. Cao-Labora, D. S. Park, M. Arjovsky, D. Worrall, C. Qin, F. Alet, B. Kozlovskii, N. Tomašev, A. Davies, P. Kohli, T. Buckmaster, B. Georgiev, J. Gómez-Serrano, R. Jiang, and C.-Y. Lai, “Discovery of Unstable Singularities,” arXiv:2509.14185 [math.AP] (2025). doi:10.48550/arXiv.2509.14185.
- [52] P. B. Allen and J. L. Feldman, “Thermal conductivity of disordered harmonic solids,” *Physical Review B* **48** (1993), 12581.

- [53] Buchert, Thomas, “On average properties of inhomogeneous fluids in general relativity: Dust cosmologies,” *Gen. Relativ. Gravit.* **32** (2000), 105–125. doi: 10.1023/A:1001800617177
- [54] Buchert, Thomas, “On average properties of inhomogeneous cosmologies,” *Gen. Relativ. Gravit.* **33** (2001), 1381–1405. doi: 10.1023/A:1012061725841
- [55] Englert, B.-G., “Fringe Visibility and Which-Way Information: An Inequality,” *Phys. Rev. Lett.* **77** (1996), 2154–2157. doi: 10.1103/PhysRevLett.77.2154
- [56] Pieter Goldau, “The Simplicity Codex” (2025). Sixteen-stage parameter-free ontology, cited as STC doi: 10.5281/zenodo.17068210
- [57] R. J. Hardy, “Energy-Flux Operator for a Lattice,” *Physical Review* **132** (1963), 168.
- [58] Iskandarani, Omar, “Swirl-String Theory (SST) Canon v0.3.4: Core Postulates, Constants, and Boxed Master Equations” (Zenodo, 2025). Single source of truth for SST symbols, constants, and canonical equations; required citation for dependent works. doi: 10.5281/zenodo.17014358
- [59] Iskandarani, Omar, “Long-Distance Swirl Gravity from Chiral Swirling Knots with Central Holes” (Zenodo, 2025). doi: 10.5281/zenodo.17155855
- [60] Iskandarani, Omar, “Swirl-String Theory (SST) Lagrangian: Emergent Relativistic EFT with Preferred Foliation” (Zenodo, 2025). doi: 10.5281/zenodo.16956665
- [61] John David Jackson, *Classical Electrodynamics* (3rd ed., Wiley, 1999).
- [62] W. Thomson (Lord Kelvin), “On vortex motion,” *Transactions of the Royal Society of Edinburgh* **25** (1869), 217–260.
- [63] Khatiwada, P. and Qian, X.-F., “Wave-particle duality ellipse and application in quantum imaging with undetected photons,” *Phys. Rev. Research* **7** (2025), 033033. doi: 10.1103/PhysRevResearch.7.033033
- [64] Particle Data Group, “Review of Particle Physics” (2024).
- [65] R. Peierls, “Zur Theorie der spezifischen Wärme,” *Annalen der Physik* **395** (1929), 1055.
- [66] Michael E. Peskin and Daniel V. Schroeder, *An Introduction to Quantum Field Theory* (Westview Press, 1995).
- [67] M. Simoncelli et al., “Unified theory of thermal transport in crystals and disordered solids,” *Nature Physics* **18** (2022), 1180.
- [68] Weinberg, Steven, “A Model of Leptons,” *Physical Review Letters* **19** (1967), 1264–1266. doi: 10.1103/PhysRevLett.19.1264
- [69] Zurek, W. H., “Decoherence, einselection, and the quantum origins of the classical,” *Rev. Mod. Phys.* **75** (2003), 715–775. doi: 10.1103/RevModPhys.75.715
- [70] G. W. Gibbons, “The Maximum Tension Principle in General Relativity,” *Foundations of Physics* **32**, 1891–1901 (2002). doi:10.1023/A:1022370717626.
- [71] M. Planck, “Über irreversible Strahlungsvorgänge,” *Annalen der Physik* **306**, 69–122 (1900). doi:10.1002/andp.19003060105.
- [72] D. J. Griffiths, *Introduction to Quantum Mechanics*, Prentice-Hall, 1995, Sec. 10.3 (classical electron radius).
- [73] P. Hořava, “Quantum Gravity at a Lifshitz Point,” *Phys. Rev. D* **79**, 084008 (2009), doi:10.1103/PhysRevD.79.084008.
- [74] T. P. Sotiriou, M. Visser and S. Weinfurtner, “Quantum Gravity without Lorentz Invariance,” *JHEP* **10**, 033 (2009), doi:10.1088/1126-6708/2009/10/033.

- [75] J. C. Maxwell, “A Dynamical Theory of the Electromagnetic Field,” *Philosophical Transactions of the Royal Society of London* **155**, 459–512 (1865). doi:10.1098/rstl.1865.0008.
- [76] H. von Helmholtz, “On Integrals of the Hydrodynamical Equations, Which Express Vortex-Motion,” *The London, Edinburgh, and Dublin Philosophical Magazine and Journal of Science* **33**, 485–512 (1867) [English translation of the 1858 German original]. doi:10.1080/14786446708639824.
- [77] W. Thomson (Lord Kelvin), “On Vortex Atoms,” *The London, Edinburgh, and Dublin Philosophical Magazine and Journal of Science* **34**, 15–24 (1867). doi:10.1080/14786446708639836.
- [78] L. D. Landau and E. M. Lifshitz, *Fluid Mechanics*, 2nd ed., Course of Theoretical Physics, Vol. 6 (Pergamon Press, Oxford, 1987).
- [79] R. L. Ricca, “Structural Complexity and Dynamical Systems,” in *Topological Fluid Mechanics*, edited volume chapter (Springer, Berlin, 2009), doi:10.1007/978-3-642-00837-5_6.
- [80] A. Einstein, “Die Grundlage der allgemeinen Relativitätstheorie,” *Annalen der Physik* **354**, 769–822 (1916). doi:10.1002/andp.19163540702.
- [81] A. Einstein, B. Podolsky, and N. Rosen, “Can Quantum-Mechanical Description of Physical Reality Be Considered Complete?” *Physical Review* **47**, 777–780 (1935). doi:10.1103/PhysRev.47.777.
- [82] A. Aspect, P. Grangier, and G. Roger, “Experimental Realization of Einstein-Podolsky-Rosen-Bohm Gedankenexperiment: A New Violation of Bell’s Inequalities,” *Physical Review Letters* **49**, 91–94 (1982). doi:10.1103/PhysRevLett.49.91.
- [83] J. C. Maxwell, *A Treatise on Electricity and Magnetism*, Clarendon Press, Oxford (1875).
- [84] W. G. Unruh, “Experimental black-hole evaporation?,” *Phys. Rev. Lett.* **46**, 1351–1353 (1981).
- [85] G. E. Volovik, *The Universe in a Helium Droplet*, Oxford Univ. Press (2003).
- [86] O. Iskandarani, “Electromagnetism as Propagating Torsion in a Hydrodynamic Vacuum: A Geometric Unification via Cartan Structure Equations,” (2025), DOI: 10.5281/zenodo.17677074.
- [87] O. Iskandarani, “Hydrodynamic Origin of the Hydrogen Ground State in Swirl-String Theory,” preprint (2025).
- [88] Russell J. Donnelly, Quantized Vortices in Helium II, Cambridge University Press, 1991.
- [89] L. D. Landau and E. M. Lifshitz, Fluid Mechanics, Course of Theoretical Physics, Vol. 6, 2nd ed., Pergamon, 1987.
- [90] W. Thomson (Lord Kelvin), On Vortex Atoms, Proc. Royal Society of Edinburgh, 1867.
- [91] E. Schrödinger, An Undulatory Theory of the Mechanics of Atoms and Molecules, *Physical Review*, 1926.
- [92] G. Călugăreanu, L’intégral de Gauss et l’analyse des noeuds tridimensionnels, *Rev. Math. Pures Appl.*, 4, 1959.
- [93] H. K. Moffatt and R. L. Ricca, Helicity and the Călugăreanu invariant, *Proc. R. Soc. Lond. A*, 439:411–429, 1992.
- [94] H. Hopf, Über die Abbildungen der dreidimensionalen Sphäre auf die Kugelfläche, *Mathematische Annalen*, 104:637–665, 1931.
- [95] J. H. C. Whitehead, An expression of Hopf’s invariant as an integral, *Proc. Natl. Acad. Sci. USA*, 33:117–123, 1947.
- [96] I. E. Dzyaloshinskii, A thermodynamic theory of “weak” ferromagnetism of antiferromagnetics, *J. Phys. Chem. Solids*, 4:241–255, 1958.

- [97] T. Moriya, Anisotropic superexchange interaction and weak ferromagnetism, *Phys. Rev.*, 120:91–98, 1960.
- [98] A. Aharoni, *Introduction to the Theory of Ferromagnetism*, Oxford University Press, 1996.
- [99] G. K. Batchelor, *An Introduction to Fluid Dynamics*, Cambridge University Press, 1967.
- [100] M. Visser, Acoustic black holes: horizons, ergospheres and Hawking radiation, *Classical and Quantum Gravity*, 15(6):1767–1791, 1998, doi:10.1088/0264-9381/15/6/024.
- [101] P. Painlevé, La mécanique classique et la théorie de la relativité, *Comptes Rendus de l'Académie des Sciences*, 173:677–680, 1921.
- [102] A. Gullstrand, Allgemeine Lösung des statischen Einkörperproblems in der Einsteinschen Gravitations-theorie, *Arkiv för Matematik, Astronomi och Fysik*, 16:1–15, 1922.
- [103] Dale Rolfsen, *Knots and Links*, Publish or Perish, 1976.
- [104] W. B. R. Lickorish, *An Introduction to Knot Theory*, Graduate Texts in Mathematics, 175, Springer, 1997.
- [105] Kunio Murasugi, *Knot Theory and Its Applications*, Birkhäuser, 1996.
- [106] Jason Cantarella, Robert B. Kusner, and John M. Sullivan, On the Minimum Ropelength of Knots and Links, *Inventiones mathematicae*, 150(2):257–286, 2002, doi:10.1007/s002220100178.
- [107] Eric J. Rawdon, Approximating the Thickness of a Knot, in *Ideal Knots*, eds. A. Stasiak, V. Katrich, L. Kauffman, World Scientific, 1998, pp. 143–150.
- [108] Roy P. Kerr, Gravitational Field of a Spinning Mass as an Example of Algebraically Special Metrics, *Physical Review Letters*, 11:237–238, 1963, doi:10.1103/PhysRevLett.11.237.
- [109] Hans Ertel, Ein neuer hydrodynamischer Erhaltungssatz, *Meteorologische Zeitschrift*, 59:271–281, 1942.
- [110] W. Wien, Ueber die Energieverteilung im Emissionsspectrum eines schwarzen Körpers, *Annalen der Physik*, 1894.
- [111] M. Planck, On the Law of Distribution of Energy in the Normal Spectrum, *Annalen der Physik*, 1901.
- [112] David J. Morin, Chapter 11: Relativity (Kinematics), 2007, Draft chapter from *Introduction to Classical Mechanics*, <https://bpb-us-e1.wpmucdn.com/sites.harvard.edu/dist/0/550/files/2023/11/cmchap11.pdf>.
- [113] A. A. Michelson and E. W. Morley, On the Relative Motion of the Earth and the Luminiferous Ether, *American Journal of Science*, 34:333–345, 1887, doi:10.2475/ajs.s3-34.203.333.
- [114] David Finkelstein and Jerrold Rubinstein, Connection between Spin, Statistics, and Kinks, *Journal of Mathematical Physics*, 9(11):1762–1779, 1968, doi:10.1063/1.1664538.
- [115] Serge Haroche and Jean-Michel Raimond, *Exploring the Quantum: Atoms, Cavities, and Photons*, Oxford University Press, 2006, ISBN:978-0198509141.
- [116] Marlan O. Scully and M. Suhail Zubairy, *Quantum Optics*, Cambridge University Press, 1997, ISBN:978-0521435956.
- [117] NIST, CODATA Recommended Values of the Fundamental Constants (2018 update), <https://physics.nist.gov/cuu/Constants/>, 2019.
- [118] Michael Tinkham, *Introduction to Superconductivity*, 2nd ed., McGraw-Hill, 1996.
- [119] John Clarke and Alex I. Braginski, *The SQUID Handbook*, Wiley-VCH, 2004.
- [120] Mark Brittenham and Susan Hermiller, Unknotting number is not additive under connected sum, arXiv e-prints, arXiv:2506.24088, 2025, doi:10.48550/arXiv.2506.24088, <https://arxiv.org/abs/2506.24088>.

- [121] W. B. R. Lickorish, An Introduction to Knot Theory, Graduate Texts in Mathematics, 175, Springer, 1997, doi:10.1007/978-1-4612-0691-0.
- [122] Kunio Murasugi, On a certain numerical invariant of link types, *Transactions of the American Mathematical Society*, 117:387–422, 1965, doi:10.2307/1994180.
- [123] Peter B. Kronheimer and Tomasz S. Mrowka, Gauge theory for embedded surfaces. I, *Topology*, 32(4):773–826, 1993, doi:10.1016/0040-9383(93)90045-U.
- [124] Jacob Rasmussen, Khovanov homology and the slice genus, *Inventiones mathematicae*, 182(2):419–447, 2004, doi:10.1007/s00222-010-0300-0.
- [125] Robion C. Kirby, Problems in low-dimensional topology, in Geometric Topology (Athens, GA, 1993), AMS/IP Stud. Adv. Math., 2:35–473, Amer. Math. Soc., 1997.
- [126] C. N. Yang and R. L. Mills, Conservation of Isotopic Spin and Isotopic Gauge Invariance, *Physical Review*, 96:191–195, 1954, doi:10.1103/PhysRev.96.191.
- [127] Sheldon L. Glashow, Partial-Symmetries of Weak Interactions, *Nuclear Physics*, 22:579–588, 1961, doi:10.1016/0029-5582(61)90469-2.
- [128] Abdus Salam, Weak and Electromagnetic Interactions, in Elementary Particle Theory: Relativistic Groups and Analyticity, ed. N. Svartholm, pp. 367–377, Stockholm, Almqvist and Wiksell, 1968.
- [129] Y. M. Cho, Restricted gauge theory, *Phys. Rev. D*, 1980.
- [130] L. Faddeev and A. J. Niemi, Partial duality in SU(2) Yang–Mills theory, *Phys. Lett. B*, 1999.
- [131] A. Zee, Quantum Field Theory in a Nutshell, 2nd ed., Princeton, 2010.
- [132] E. Witten, An SU(2) anomaly, *Phys. Lett. B*, 1982.
- [133] S. Weinberg, The Quantum Theory of Fields, Vol. II, Cambridge, 1996.
- [134] M. E. Peskin and D. V. Schroeder, An Introduction to Quantum Field Theory, Westview, 1995.
- [135] F. Englert and R. Brout, Broken Symmetry and the Mass of Gauge Vector Mesons, *Phys. Rev. Lett.*, 13:321–323, 1964, doi:10.1103/PhysRevLett.13.321.
- [136] P. W. Higgs, Broken Symmetries and the Masses of Gauge Bosons, *Phys. Rev. Lett.*, 13:508–509, 1964, doi:10.1103/PhysRevLett.13.508.
- [137] Eduardo Fradkin, Field Theories of Condensed Matter Physics, 2nd ed., Cambridge University Press, 2013.
- [138] Xiao-Gang Wen, Quantum Field Theory of Many-Body Systems, Oxford University Press, 2004.
- [139] H. P. Greenspan, The Theory of Rotating Fluids, Cambridge University Press, 1968.
- [140] Geoffrey K. Vallis, Atmospheric and Oceanic Fluid Dynamics, 2nd ed., Cambridge University Press, 2017, doi:10.1017/9781107588417.
- [141] L. D. Landau and E. M. Lifshitz, Fluid Mechanics, Course of Theoretical Physics, Vol. 6, Pergamon, 1987.
- [142] M. J. Lighthill, Waves in Fluids, Cambridge University Press, 1978.
- [143] L. Brillouin, Wave Propagation and Group Velocity, Academic Press, 1960.
- [144] B. P. Abbott et al. (LIGO Scientific Collaboration and Virgo Collaboration), GW170817: Observation of Gravitational Waves from a Binary Neutron Star Inspiral, *Physical Review Letters*, 119:161101, 2017, doi:10.1103/PhysRevLett.119.161101.

- [145] B. P. Abbott et al., Gravitational Waves and Gamma-Rays from a Binary Neutron Star Merger, *The Astrophysical Journal Letters*, 848:L13, 2017, doi:10.3847/2041-8213/aa920c.
- [146] M. P. Brenner, S. Hilgenfeldt, and D. Lohse, Single-bubble sonoluminescence, *Reviews of Modern Physics*, 74:425–484, 2002, doi:10.1103/RevModPhys.74.425.
- [147] D. J. Flannigan and K. S. Suslick, Measurement of pressure and density inside a single sonoluminescing bubble, *Physical Review Letters*, 96:204301, 2006, doi:10.1103/PhysRevLett.96.204301.